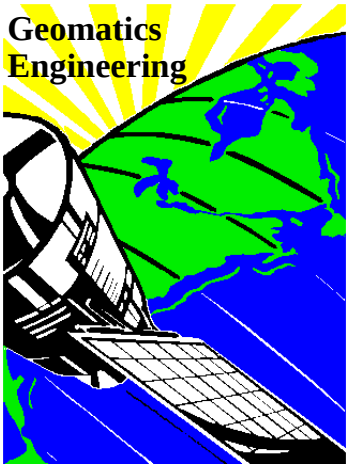


**UCGE REPORTS**
**Number 20055**

**Department of Geomatics Engineering**

# Precise GPS Positioning in the Marine Environment

**by**

**Congyu Liu**

**December 1993**


**(www.geomatics.ucalgary.ca/GradTheses.html)**

THE UNIVERSITY OF CALGARY

# PRECISE GPS POSITIONING IN THE MARINE ENVIRONMENT

BY

CONGYU LIU

A THESIS

SUBMITTED TO THE FACULTY OF GRADUATE STUDIES

IN PARTIAL FULFILLMENT OF THE REQUIREMENTS FOR THE

DEGREE OF MASTER OF SCIENCE IN ENGINEERING

DEPARTMENT OF GEOMATICS ENGINEERING

CALGARY, ALBERTA

DECEMBER, 1993

## PREFACE

This is an unaltered version of the author's Master of Science in Engineering Thesis of the same title. This thesis was accepted by Faculty of Graduate Studies in December, 1993.

The faculty supervisor for this work was Dr. Gérard Lachapelle and the other member of the examining committee were Dr. M.E. Cannon, Dr. R. Li and Dr. D.H. Manz.

## ABSTRACT

Differential GPS kinematic positioning using P code and narrow correlator spacing C/A code technologies in the marine environment is investigated with emphasis on a high level of accuracy. Theory of GPS observables and error sources are reviewed and analyzed. Two processing methods, namely, carrier phase ambiguity resolution on the fly and carrier phase smoothing of the code, are presented. A variation of the least-squares ambiguity search technique is applied in three kinematic tests, namely two shipborne cases and a land vehicle case. In order to improve the on-the-fly ambiguity resolution time and reliability with single frequency receivers, a quadruple receiver system consisting of two static monitor units and two mobile remote units mounted on the mobile platform is developed. Results of this system are analyzed and assessed. The application for water level profiling with a cm-level accuracy is also investigated using GPS carrier phase observations with the ambiguities resolved on the fly. Agreement between GPS-derived and levelled orthometric heights at Bench Marks along the shores of the river is reached at 6.4 cm RMS.

## ACKNOWLEDGEMENTS

I wish to express my sincere appreciation to my supervisor, Professor Gérard Lachapelle, for his continuous support, encouragement and guidance throughout the course of my graduate studies.

Special thanks are extended to Professor M. Elizabeth Cannon, Mr. Gang Lu and Mr. Weigen Qiu for providing software SEMIKIN™, C³NAV™ and FLYKIN™ used in these investigations as well as for the many fruitful discussions related to my research. Mr. Bryan Townsend, Mr. Gang Lu, Mr. Dingsheng Chen and Mr. Weigen Qiu are all thanked for their assistance in data collection. Appreciation should also go to many of my colleagues in the GPS group, Messrs. Gang Lu, Dingsheng Chen, Weigen Qiu, Huangqui Sun , and Jing Shi for sharing their knowledge in GPS and computer systems. Mr. Legary is gratefully acknowledged for proofreading the manuscript. Dr. Ron Li and Dr. D.H. Manz are thanked for their valuable advice on this thesis.

Parts of my graduate studies was financially supported through grants and contracts from the Natural Science and Engineering Research Council and the Canadian Hydrographic Service, respectively. Their contribution is gratefully acknowledged.

Finally, thanks go to my wife, Paula, and my daughter, Ellen, for sharing the troubles and pleasures of a graduate student.

## TABLE OF CONTENTS

Page

## LIST OF TABLES

## LIST OF FIGURES

## NOTATION

### i) Symbols

| | |
|---|---|
| $a_0$ | satellite clock time offset |
| $a_1$ | frequency offset |
| $a_2$ | frequency drift |
| c | speed of light |
| dt | satellite clock error |
| dT | receiver clock error |
| $d_{ion}$ | ionospheric bias |
| $d_{trop}$ | tropospheric delay |
| $d\rho$ | orbit errors |
| f | frequency |
| h | ellipsoidal height |
| H | orthometric height |
| L1 | GPS carrier with frequency of 1575.42 MHz |
| L2 | GPS carrier with frequency of 1227.60 MHz |
| N | carrier phase integer ambiguity, or |
| N | geoidal height |
| P | pseudorange observation, or |
| P | surface pressure in standard atmospheres |
| $r_s$ | distance from the center of the earth to the station |
| t | measurement transmit time |
| T | surface temperature |
| ^ | denotes estimated quantity |
| $\rho$ | range between the receiver and the satellite |

| | |
|---|---|
| $\Phi$ | carrier phase observation (m) |
| $\lambda$ | carrier phase wavelength |
| $\varepsilon(p)$ | measurement noise |
| $\varepsilon(p_{rx})$ | receiver pseudorange noise |
| $\varepsilon(p_{mult})$ | multipath effects in pseudorange |
| $\varepsilon(\Phi)$ | carrier phase noise |
| $\varepsilon(\Phi_{rx})$ | receiver carrier phase noise |
| $\varepsilon(\Phi_{mult})$ | multipath effects in carrier phase |

**ii) Defined Operators**

| | |
|---|---|
| $C^{-1}$ | matrix inverse |
| | single difference between satellites |
| $\Delta$ | single difference between receivers |
| $\nabla\Delta$ | double difference |
| nint(•) | nearest integer of |
| $\prod$ | product of |
| $\Sigma$ | summation of |
| $\dot{(\ )}$ | derivative with respect to time |

**iii) Acronyms**

| | |
|---|---|
| AFM | Ambiguity Function Method |
| B.M.'s | Bench Marks |
| CHS | Canadian Hydrographic Service |
| C/A | Coarse Acquisition code |
| DD | Double Difference |
| DGPS | Differential GPS |
| GDOP | Geometry Dilution of Precision |

| | |
|---|---|
| GPS | Global Positioning System |
| LSAST | Least-Squares Ambiguity Search Technique |
| OTF | On The Fly |
| P code | Precise acquisition code |
| PDOP | Positional Dilution of Precision |
| RMS | Root Mean Square |
| SA | Selective Availability |
| SPS | Standard Positioning Service |
| TEC | Total Electron Content |

CHAPTER 1

# INTRODUCTION

## 1.1 BACKGROUND AND OBJECTIVE

GPS positioning is required for a variety of hydrographic and other applications. Precise positioning of a moving ship is especially challenging due to the high dynamics of the antenna and the high reflectivity of the water. The capabilities of GPS for shipborne applications have been extensively investigated. The estimates of relative pseudo-range positioning can be achieved with accuracies of 3m to 10m (e.g., Wells et al 1986). The use of carrier phase smoothing techniques with standard C/A code receivers has resulted in RMS accuracies at the 1-3 m level (e.g., Lachapelle et al 1988). If accuracies are required at the sub-metre or centimetre level, the receivers and/or the data processing techniques must be improved.

In order to achieve the centimetre level accuracy, carrier phase measurements must be employed. Carrier phase measurements are precise but they are ambiguous because the number of whole cycles (ambiguity) between the satellite and the receiver is unknown. Thus, this unknown cycle ambiguity of

carrier phase observation must be correctly resolved when high kinematic positioning is required.

Ambiguity resolution on the fly is not easy to achieve. It relies on a lot of factors, such as ambiguity search techniques, a change in receiver and satellite geometry, and the effects of the observation errors (e.g., Abidin, 1992). In the marine environment, the ship dynamics is generally more turbulent, cycle slips are more frequent, multipath caused by the ship's reflective structure and sea water is much larger, and the ship can never be static even if anchored in the harbour. Therefore, on-the-fly ambiguity resolution is more challenging at the beginning of the session, cycle slip occurrences as well as on occasions when the rising of a new satellite will be included in the positioning process.

Over the past few years, various ambiguity search techniques have been developed. These techniques include P code aided ambiguity resolution (Wubbena, 1989; Abidin et al, 1990), the ambiguity function methods (Counselman and Gourevitch, 1981; Remondi, 1984, 1991), and the least squares ambiguity search technique (Hatch, 1991; Lachapelle et al 1992, 1993a,1993b).

The P-code aided ambiguity resolution technique requires P code and L1/L2 carrier phase measurements. The linear combinations of carrier phase measurements result in wide-lane and narrow-lane carrier phase for ambiguity resolution process (Abidin et al, 1990). There are however three possible problems. Firstly the P-code is scheduled to be unavailable for civilian use upon completion of the full GPS constellation (McNeff,1992). Secondly, pseudoranges are affected to a larger level by multipath and receiver noise than carrier phase measurements. Under realistic conditions, there may be some difficulties in

resolving the integer ambiguities with confidence using pseudoranges alone. The third problem is that the effects of the ionospheric errors are more sensitive in the wide-lane observables.

The ambiguity function was first introduced in GPS data processing by Counselman and Gourevitch (1981). This technique for kinematic and pseudo-kinematic applications has been thoroughly investigated (see for instance, Mader, 1990; Remondi, 1991; Lachapelle et al, 1992). It is used to measure the level of agreement among observations from satellites. It has the advantage being of free from cycle slips. But it requires an intensive computation and the discrimination between the right solution and false solutions sometime is not robust (Hatch,1991). The studies of the on the fly ambiguity resolution results using the ambiguity function technique for precise sea level measurements can be found in (Kelecy et al, 1992).

The least-squares ambiguity search technique was proposed by Hatch (1991). This method uses differential code measurements to estimate an approximation for the mobile receiver to limit the potential number of integer ambiguity solutions. Then, a least-squares search technique is used to isolate the correct integer ambiguity combination. Four primary satellites are required to generate an entire set of potential solutions and redundant secondary satellites to identify the proper solution by the estimation of minimum variance factor. Therefore, the least-squares ambiguity search technique is considered as a measure of disagreement among the observations. Both the least-squares ambiguity search technique and ambiguity function method were found to be mathematically equivalent (Lachapelle et al 1992).

Some other ambiguity resolution techniques have also been tested. Landau and Euler (1992) used a sequential square root information filter to conduct ambiguity resolutions. It is reportedly very fast and is suited for real time applications. Abidin (1992) proposed an integrated search technique as the best solution. Chen (1993) developed a fast ambiguity search filter based on the concept of recursive computation of the search range of the ambiguities in the filtering process of ambiguity resolution.

The ambiguity search method selected in this thesis is the least-squares approach as described and implemented by Lachapelle et al (1992). Two properties of the least squares search are employed. One is that only three of the double difference carrier phase ambiguities are independent. The second property is that the estimated variance factor calculated using the adjusted carrier phase residuals should be minimum at the correct solution. Performance of ambiguity resolution on the fly using dual frequency Ashtech P code and single frequency NovAtel narrow correlator spacing C/A code technologies are investigated in this thesis.

The objective of this thesis is to investigate the performance of narrow correlator spacing single frequency C/A code and dual frequency P code technologies for precise DGPS positioning in the marine environment. Two processing methods, namely carrier phase ambiguity resolution on the fly and carrier phase smoothing code, are employed. On-the-fly ambiguity resolution with multi-receiver configuration is also studied to speed up the ambiguity search process and to increase its reliability. Three kinematic test cases are used in the analysis, namely two shipborne cases and a land mode case. The land case consists of a quadruple receiver system to demonstrate the feasibility of

ambiguity resolution with such a multi-receiver configuration for speeding up the ambiguity search process. Survey launch tests are used to investigate precise DGPS positioning with the NovAtel GPSCard™ and Ashtech P-XII receivers in the marine environment.

## 1.2 OUTLINE OF THESIS

In Chapter 2, the fundamental aspects of GPS and kinematic positioning are reviewed. The basic GPS observables and measurement models are presented, observation error sources are described, and the differential GPS technique to mitigate the error effects is outlined.

Chapter 3 describes the concepts and mathematical methodologies of two processing methods employed in this research, namely carrier phase smoothing of code and carrier phase ambiguity resolution on the fly. The concept of ambiguity resolution on the fly with multi-receiver configuration is introduced.

Chapter 4 concentrates on kinematic results in the marine environment. The field tests conducted and data sets used are described. Code multipath and ionospheric effects are analyzed. Performance of ambiguity resolution on the fly using narrow correlator spacing single frequency C/A code and dual frequency P code technologies are investigated. The kinematic positioning results of carrier phase solution, code solution and carrier phase smoothed code solution are assessed and inter-compared.

In Chapter 5, a quadruple receiver system consisting of two static monitor units and two mobile remote units for ambiguity resolution is investigated. Field tests in land mode conducted on two different occasions are described. The time to resolution with the multi-receiver configuration is compared with single pairs of units. The semi-kinematic results are analyzed and discussed.

Presented in Chapter 6 is an application of GPS to the water level profiling of Fraser River, British Columbia. Field works conducted and data preprocessing are described. The DGPS static survey results for monitor stations are given and triangle misclosures for the baseline solutions are also analyzed. The kinematic water level profiling results are presented. The differences between GPS derived heights and leveled heights at bench marks along the river are investigated. The accuracy of water level profiles is discussed. The performance of water level profile for long distance solutions between GPS reference station and survey launch is also investigated.

Chapter 7 contains the main conclusions of the thesis and recommendations for further investigations.

CHAPTER 2

# GLOBAL POSITIONING SYSTEM AND MEASUREMENT MODELS

Outlined in this chapter are the GPS concepts and the fundamental models. The basic aspects of GPS are reviewed. The GPS measurement models and error sources are then described. Finally, the differential GPS positioning technique is summarized.

## 2.1 GENERAL DESCRIPTION OF THE GLOBAL POSITIONING SYSTEM

The Global Positioning System (GPS) is a satellite-based radio positioning system designed for accurate navigation. It uses radio signals from satellites to determine the three-dimensional positions of users. This system is composed of a space segment, a control segment and a user segment. The space segment contains the satellites that broadcast the ranging signals. The control segment consists of the ground monitor stations that perform the satellite tracking, orbit

determination and time synchronization. The user segment is made up of the GPS receivers that translate the satellite ranging signals into a navigation solution.

Upon completion in 1994, the GPS constellation will involve 21 operating satellites plus three spares (see Figure 2.1). These satellites are placed in six different orbital planes at an altitude of 20,000 km above the earth. It is an all-weather system providing 24 hour world-wide satellite coverage with a minimum of four satellites in view simultaneously.

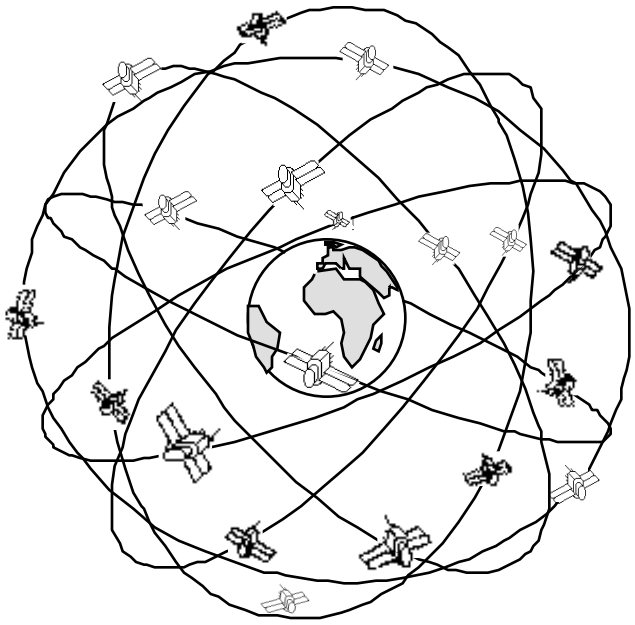

**Figure 2.1 GPS Satellite Configuration**

The GPS satellites continuously transmit signals on the frequencies; L1=1575.42 MHz and L2=1227.6 MHz. The associated wavelengths of the L1 and L2 carriers are approximately 19 cm and 24 cm, respectively. These carriers are modulated with two types of code, namely the Clear Acquisition (C/A) code and

the Precise (P) code. The L1 carrier is modulated with both the C/A and P code, and the L2 carrier is modulated with the P code only. In addition, a navigation message is also modulated on the carriers. The use of two kinds of code provides two different accuracies to users. Two frequency signals can be used for the correction of ionospheric effects on GPS measurements.

The concept of positioning with GPS is based on simultaneous ranging to at least four GPS satellites to determine the unknown coordinates of a point (Figure 2.2). From a geometric point of view, a unique solution can be obtained if the distances from three satellites with known coordinates are measured. Because the GPS satellite clocks cannot be synchronized with the user clock, a fourth unknown (the clock bias) is introduced. Therefore, a minimum of four satellites are used to determine the three-dimensional position vector.

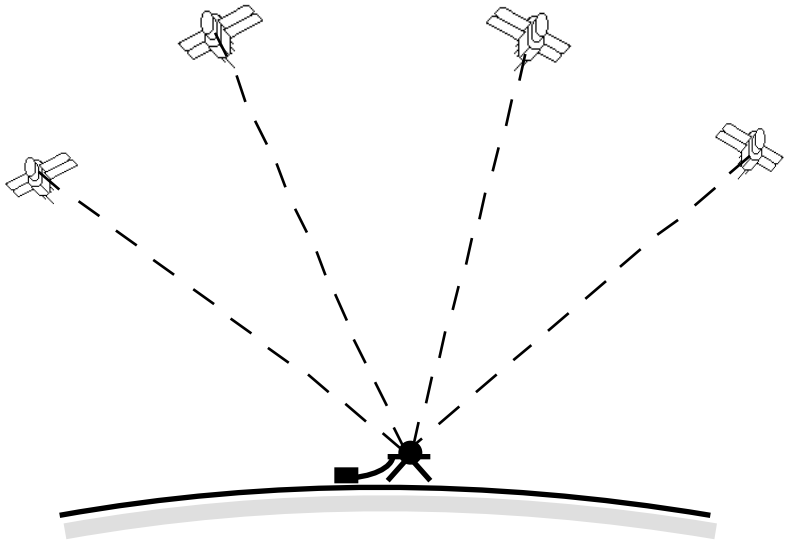

**Figure 2.2 Absolute GPS Positioning**

The determination of point coordinates is affected by many errors discussed later in this chapter. The single point positioning accuracy of the

Standard Positioning Service (SPS) is 20 to 30 m when Selective Availability (SA) is turned off (Lachapelle et al, 1991a). Selective Availability is effected through satellite clock dithering and broadcast orbit ephemeris degradation. When Selective Availability is turned on, the accuracy is reduced to the 100 m (2 drms) horizontal and 156 m (2 $\sigma$) vertical. The method of single point positioning cannot generally meet precise positioning requirements. The differential GPS positioning method can, however, significantly reduce the above errors.

Differential GPS positioning, also called relative positioning, involves simultaneous occupation and tracking of satellites from a known point station and from a mobile platform (Figure 2.3). This method exploits the fact that GPS positioning errors are spatially correlated within a certain distance. Differential GPS positioning may be done using several methods. Differential range corrections may be calculated by comparing the observed and predicted values at the known point station and then applying these corrections to the observations at the mobile platform. Alternatively, the common GPS positioning errors may be cancelled by differencing between simultaneous observations at the known point and the mobile platform. Both methods provide similar results and determine the relative position of the trajectory with respect to the fixed known station. The rms accuracies of differential GPS positioning are 2 m to 5 m for code only, 0.5 m to 2 m for carrier phase smoothed code, and better than 10 cm for carrier phase solution when the separation between the monitor and remote is less than 50 km (Lachapelle et al, 1991a).

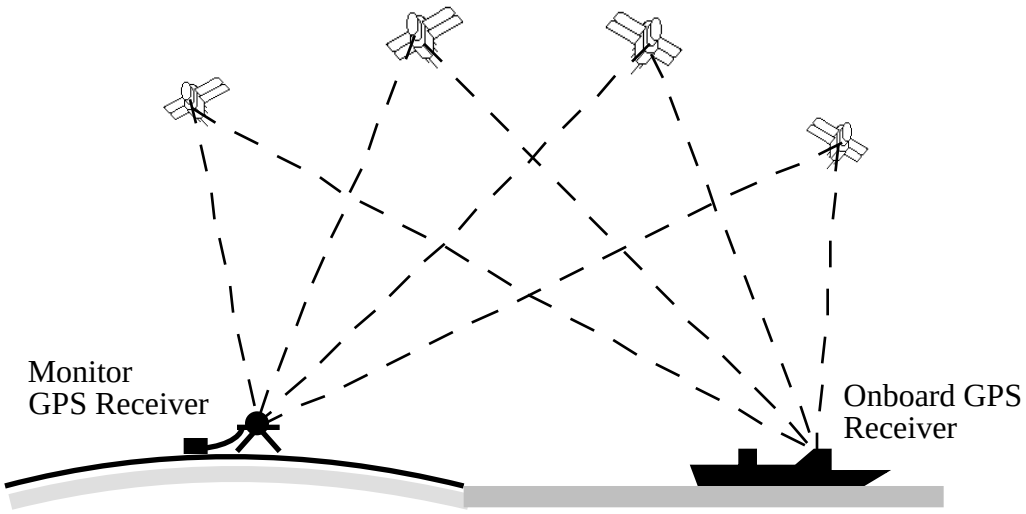


**Figure 2.3 Differential GPS Positioning**

## 2.2 GPS MEASUREMENT MODELS

Generally speaking, there are three basic GPS observations, namely pseudorange, carrier phase and phase rate (also called Doppler frequency).

Pseudorange observation is the time delay between the transmission time and the reception time of the satellite signals. The range between the receiver and satellite is obtained by multiplying the transit time by the speed of light. The pseudorange observation equation can be written as (Lachapelle, 1991b):

$$p = \rho + d\rho + c\,(dt - dT) + d_{ion} + d_{trop} + \varepsilon(p) \qquad (2.1)$$

where $p$ ... is the pseudorange observation (m)

$\rho$ ... is the range between the receiver and the satellite (m)

$d\rho$ ... is the orbit error (m)

$c$ ... is the speed of light in vacuum (m/s)

$dt$ ... is the satellite clock error (s)

$dT$ ... is the receiver clock error (s)

$d_{ion}$ ... is the ionospheric delay(m)

$d_{trop}$ ... is the tropospheric delay (m)

$\varepsilon(p)$ ... is the measurement noise (m).

The code measurement noise $\varepsilon(p)$ contains code receiver noise $\varepsilon(p_{rx})$ and multipath $\varepsilon(p_{mult})$. It can be expressed as (Lachapelle, 1991b):

$$\varepsilon(p) = f\{\varepsilon(p_{rx}), \varepsilon(p_{mult})\} \qquad (2.2)$$

where $\varepsilon(p_{rx})$ ... is the receiver pseudorange noise (m)

$\varepsilon(p_{mult})$ ... is the multipath effect in pseudorange (m).

Carrier phase observation is the difference between the phase of the incoming carrier signal from the satellite and the phase of a carrier signal generated by receiver oscillator. The difference, which is the beat frequency, is due to the Doppler effect caused by the relatiove motion between the satellite and observation point. The carrier phase measurement equation is given as (Lachapelle, 1991b):

$$\Phi = \rho + d\rho + c\,(dt - dT) + \lambda N - d_{ion} + d_{trop} + \varepsilon(\Phi) \qquad (2.3)$$

where $\Phi$ ... is the carrier phase observation (m)

$\lambda$ ... is the carrier phase wavelength (m/cycle)

$N$ ... is the carrier phase integer ambiguity (cycles)

$\varepsilon(\Phi)$ ... is the carrier phase noise (m)

$\rho$, $d\rho$, $c$, $dt$, $dT$, $d_{ion}$, $d_{trop}$ are the same as in Eqn. (2.1).

Similar to code measurement noise, the carrier phase measurement noise $\varepsilon(\Phi)$ is also a function of receiver noise $\varepsilon(\Phi_{rx})$ and multipath $\varepsilon(\Phi_{mult})$, i.e.,

$$\varepsilon(\Phi) = f\{\varepsilon(\Phi_{rx}), \varepsilon(\Phi_{mult})\} \tag{2.4}$$

where $\varepsilon(\Phi_{rx})$ ... is the receiver carrier phase noise (m)

$\varepsilon(\Phi_{mult})$ ... is the multipath effects in carrier phase (m).

Comparing Eqn. (2.1) with Eqn. (2.3), it is seen that both pseudorange and carrier phase measurements are similar except for the ambiguity term $\lambda N$, the sign of the ionospheric correction term $d_{ion}$, and the noise of $\varepsilon(p)$ and $\varepsilon(\Phi)$. The two observations have a different level of accuracy. The carrier phase observation has a much lower receiver noise and multipath effect than the pseudorange observation and thus a higher accuracy, but it is ambiguous because the integer value of the carrier phase ambiguity N cannot be known in advance. It is not an easy task to determine the ambiguity even in the case of static positioning. A discussion of ambiguity resolution on the fly is found in next Chapter.

A third fundamental GPS observation is the Doppler frequency which is simply the time derivative of the carrier phase. The Doppler frequency is measured on the pseudorange. The model for GPS the Doppler frequency measurement can be written as:

$$\dot{\Phi} = \dot{\rho} + \dot{d}\rho + c(\dot{dt} - \dot{dT}) - \dot{d}_{ion} + \dot{d}_{trop} + \varepsilon(\dot{\Phi}) \tag{2.5}$$

where $\dot{(\ )}$ ... denotes a time derivative.

As shown in Eqn. (2.5), the Doppler frequency is not a function of the carrier phase ambiguity. Thus it is free from cycle slips and is usually used for estimation of the receiver velocity. From the mathematical models of GPS observations discussed before, it is noted that GPS measurements are subject to a number of errors, which will be described in Section 3.

## 2.3 ERROR SOURCES

The errors in GPS observations include receiver noise, multipath, tropospheric and ionospheric delays, satellite and receiver clock errors, and orbital errors. They are discussed in the following subsections.

### 2.3.1 Receiver Noise

Receiver measurement noise includes the thermal noise intercepted by the antenna or generated by the internal components of the receiver (Martin, 1980). It is affected by many parameters, such as, the tracking bandwith, the signal to noise density and code tracking mechanization parameters. Usually, manufacturers claim that the noise levels are respectively 1 m for C/A code pseudorange, 10 cm for P code pseudorange and 5 mm for carrier phase. It should be mentioned that NovAtel GPSCard™, through the narrow correlator spacing code tracking loop technology employed, can achieve 10 cm accuracy for C/A code pseudorange.

### 2.3.2 Multipath

Multipath is the phenomena where the reception of signals is reflected by objects and surfaces in the environment around the antenna. Multipath error affects both pseudorange and carrier phase measurements. The amount of multipath error for code observation is much larger than carrier phase multipath error. Pseudorange multipath can reach up to one chip length of the PRN code, i.e., 293 m for the C/A code, and 29.3 m for the P code; while carrier phase multipath is less than 25 % the carrier phase wavelength, e.g., approximate 5 cm for L1 carrier phase (Georgiadou and Kleusberg, 1989). The multipath is also proportional to the ratio of the direct signal power to the reflected signal power. Typically, in static case, multipath is non-gaussian in nature and shows sinusoidal oscillations with periods of a few minutes. In kinematic mode, multipath is more random owing to vehicle movement and the environment change. Even in the case where multipath is considered as random, it will still result in additional measurement noise of several metres (Lachapelle et al, 1989). Especially in the marine environment, multipath is greater due to ship reflective structure and sea water. Hence, multipath is the dominant error source for applications of shipborne GPS positioning.

There are several techniques for reduction of multipath error. The most direct and simple approach is careful selection of the antenna site and special antenna design; for example, using a chokering groundplane can significantly mitigate the multipath error. The second much used technique is temporal averaging. This technique can effectively remove multipath signatures, but it does not work well for multipath from nearby objects. The third method is to calibrate pseudorange multipath by using a linear combination of carrier phase

observables. Carrier phase measurements are two orders of magnitude less noisy than code measurements in terms of multipath effect. The combined carrier phase with code can reduce the pseudorange multipath effects. The last method discussed here is using the narrower lag spacing to mitigate the multipath. This technique does a very good job especially for the C/A code (Van Dierendonck, et, al, 1992).

### 2.3.3 Tropospheric Delay

The tropospheric delay is caused by the refraction of a GPS signal in lower atmosphere (the layer from the earth surface to approximately 60 km). The magnitude of tropospheric delay is affected by a number of parameters, such as, the temperature, humidity, pressure, the height of the user, and the type of terrain below the signal path.

The effect of the troposphere is usually considered as a mixture of a dry and a wet component. The dry component contributes about 80 % to 90 % of the total tropospheric refraction and can be modeled with an accuracy of 1 % to 2 % at the zenith. The wet component is only some 10 % - 20 % of the total tropospheric refraction and cannot be estimated accurately due to the variability of water vapour. When elevation angle of satellite decreases (below $10^{\circ}$), the tropospheric delay will be much greater and will be estimated with much less accuracy. It will result in a lower position accuracy. This is one major reason why satellites with elevation angles greater than $10^{\circ}$ are used for precise static and kinematic GPS positioning.

There have been numerous studies performed in the creation and testing of tropospheric models (Hopfield, 1969; Saastamoinen, 1973; Black, 1978). The Black model is a very easy one and is expressed as (Black, 1978):

$$\Delta S = \Delta S_d + \Delta S_w \quad (2.6)$$

$$\Delta S_d = 2.34\ P \cdot [\ (T - 4.12) / T\ ] \cdot\ I\ (h = h_d, E\ ) \quad (2.7)$$

$$\Delta S_w\ = k_w \cdot I\ (h = h_w, E\ ) \quad (2.8)$$

$$I\ (h = h, E\ ) = \{\ 1 - [(\cos E) / (1 + (1 - l_c)h / r_s)]^2\ \}^{-1/2} \quad (2.9)$$

$$h_d = 148.98\ (T - 4.12)\ \text{m} \quad \text{above the station} \quad (2.10)$$

$h_w = 13{,}000$ m

$l_c = 0.85$

$k_w = 0.28$ for summer in tropics or mid-latitudes

0.20 for spring or fall in mid-latitudes

0.12 for winter in maritime mid-latitudes

0.06 for winter in continental mid-latitudes

0.05 for polar regions

$r_s$ distance from the center of the earth to the station

P surface pressure in standard atmospheres

T surface temperature

### 2.3.4 Ionospheric Effect

The ionosphere is a layer of the atmosphere which is roughly 50 to 1000 km above the Earth's surface. It is composed of a sufficient concentration of free electrons to affect electromagnetic waves significantly. GPS signals traveling through the ionosphere are affected by refraction and dispersion. The refractive

group index of the ionosphere is greater than 1, which means that the group velocity of radio waves is smaller than the speed of light in vacuum. The refractive phase index of the ionosphere is smaller than 1, so the phase velocity of radio waves is greater than the speed of light in vacuum. These cause delay on the measured pseudorange and advance on the measured carrier phase. Therefore, the ionospheric corrections are the opposite sign on pseudorange and carrier phase observations, respectively.

The ionospheric effect is proportional to the Total Electron Content (TEC) along the propagation path and can be expressed as (Klobuchar, 1983):

$$\Delta t = \textbf{Error!} \mathrm{TEC} \qquad (2.11)$$

where c ... is the speed of light

f ... is the frequency

TEC ... is the Total Electron Content or columnar electron density in el $m^{-2}$ (nbr of electrons in a column of 1m x 1m )

The above equation shows that the ionospheric delay is dependent on TEC. The TEC varies with solar ionizing flux, magnetic activity, sunspot cycle, season, time of day, user location and satellite elevation angle. The amount of ionospheric error may range from more than 150 m (at midday, during periods of intense sunspot activity, with the satellite at low elevation) to less than 5 m (at night, during periods of minimum sunspot activity, with the satellite at the zenith) (Wells et al, 1986).

One way to assess ionospheric effect is by taking dual frequency measurements and using the dispersive nature of the ionosphere to eliminate the ionospheric error. The group delay and carrier phase advance can be estimated as (Wells et al, 1986):

$$d\,\rho_{ion} = [\,\rho(L1) - \rho(L2)\,]\ \textbf{Error!} \qquad (2.12)$$

$$d\,\Phi_{ion} = \textbf{Error!}\,[\,\Phi(L1) - \textbf{Error!}\,\Phi(L2) - (N_1 - \textbf{Error!}\,N_2)\,] \qquad (2.13)$$

where $d\rho_{ion}$, $d\Phi_{ion}$ ...are the ionospheric corrections to the L1 pseudorange and carrier phase measurements

$\rho(L1)$, $\rho(L2)$ ... are the L1 and L2 pseudorange measurements

$\Phi(L1)$, $\Phi(L2)$ ... are the L1 and L2 carrier phase measurements

$f_1$, $f_2$ ... are the L1 and L2 frequencies

$N_1$, $N_2$ ... are the ambiguities on L1 and L2

Strictly speaking, the carrier phase ionospheric correction at a specific epoch cannot be determined due to the unknown ambiguities $N_1$, $N_2$. Only the differential ionospheric correction can be calculated if both L1 and L2 are tracked over a time interval ($t_1$, $t_2$) without any cycle slips. The technique using dual frequency correction can be expected to remove most the ionospheric error. However, during mid-afternoons and high solar activity cycle, this correction may not be adequate for certain applications (Wells et al, 1986).

Differencing observations from one satellite between two stations can reduce ionospheric effect since the ionospheric delay is to same extent spatially correlated between the stations. The another technique is to use the broadcast

model for reducing the ionospheric error. About 50 % of this delay can be removed by application of the standard ionospheric model (Klobuchar, 1983). As well, Weigen et al (1993) applies a least-squares technique to estimate the error of the ionosphere with single frequency measurements based on the opposite signs of the group delay and carrier phase advance.

### 2.3.5 Satellite and Receiver Clock Errors

The satellite clock error is the difference of satellite clock time with respect to true GPS time. The relationship between a specific clock time and GPS time is transmitted by the Control Segment through a three parameter model (Wells et al, 1986)

$$\Delta t_{sv} = a_0 + a_1 ( t - t_0 ) + a_2 ( t - t_0 )^2 \qquad (2.14)$$

where $\Delta t_{sv}$ ... is the difference between satellite clock time and GPS time

$t$ ... is the measurement transmit time

$t_0$ ... is the reference time

$a_0$ ... is the satellite clock time offset

$a_1$ ... is the frequency offset

$a_2$ ... is the frequency drift

GPS satellites carry atomic clock which maintain a highly accurate GPS time in orbit. However, the accuracy is degraded by Selective Availability (SA). SA includes satellite clock dithering which is implemented through the injection of errors in the $a_1$ term and reduces the accuracy from the sub 100 nanosecond

level to 300 nanoseconds (Dewey, 1992). When the difference from a satellite to two receivers is performed, the satellite clock error is removed.

Receiver clock error is the offset of the receiver clock time with respect to GPS time. In general, geodetic receivers are synchronized with GPS time before observation sessions, but the synchronization to a fraction of a millisecond is possible. As well, the receiver clock may drift after synchronization. Since the error is dependent on receiver hardware, it can be estimated as an unknown parameter or eliminated by differencing from one receiver to two satellites.

### 2.3.6 Orbital Error

The orbital error arises from the uncertainties of the predicted broadcast ephemerides and Selective Availability (SA). The broadcast ephemerides of the satellites are updated by GPS Control Segment. In order to generate the navigation messages of the satellites, monitoring stations distributed around the world are required to continuously track all satellites in view. Then, this data is transmitted to the master station and processed to create up-to-date navigation parameters. It is estimated that broadcast ephemerides error is about 20 metres. When post-mission precise ephemerides replace the broadcast ephemerides, the precise orbits are accurate at the 5 metre level.

In addition to satellite clock dithering discussed above, SA is also implemented by degrading satellite orbital information to deny unauthorized real-time use of full GPS position and velocity accuracy. It is estimated that the accuracy may decrease to 100 m (2 drms) when SA is turned on.

## 2.4 DIFFERENTIAL GPS TECHNIQUES

The fundamental model equations for pseudorange, carrier phase and Dopller frequency involve bias terms related to satellite and receiver clock errors, orbital error and atmospheric effects. It is found that many of these errors are spatially correlated between the receivers tracking simultaneous satellites. Some errors are to a certain extent satellite dependent, such as orbital, atmospheric and satellite clock errors; some errors are receiver dependent, such as receiver clock errors. Differencing GPS observations ('between-satellite', or 'between receiver' , and both 'between-receiver' and 'between-satellite') are used to eliminate or effectively reduce the common errors.

The single 'between receiver' difference (see Figure 2.4) can be performed by differencing the GPS observations from two receivers to one satellite. The single difference equations for the pseudorange, carrier phase and Dopller frequency are (Lachapelle, 1991b):

$$\Delta p = \Delta\rho + d\Delta\rho - c\Delta dT + \Delta d_{ion} + \Delta d_{trop} + \Delta\varepsilon(p) \qquad (2.15)$$

$$\Delta\Phi = \Delta\rho + d\Delta\rho - c\Delta dT + \lambda\Delta N - \Delta d_{ion} + \Delta d_{trop} + \Delta\varepsilon(\Phi) \qquad (2.16)$$

$$\Delta\dot{\phi} = \Delta\dot{\rho} + \Delta\dot{d}\rho + c\Delta\dot{d}T - \Delta\dot{d}_{ion} + \Delta\dot{d}_{trop} + \Delta\varepsilon(\dot{\phi}) \qquad (2.17)$$

where $\Delta$ ... denotes a single difference operator between receivers

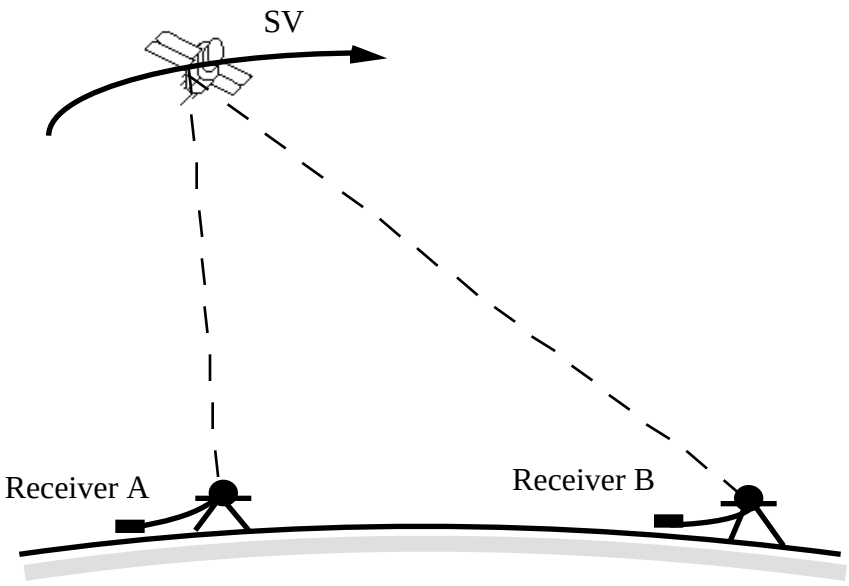


**Figure 2.4 Single Differencing Between Receivers**

In the single difference observables, the satellite clock error has been vanished and the residual orbital and atmospheric effects have been reduced and can be neglected for stations separated less than 30 km under normal atmospheric conditions. The relative receiver clock error, however, may be significant and must be estimated, along with the parameters of position, velocity and carrier phase ambiguity. To eliminate the receiver clock error, double difference between receivers and between satellites (shown in Figure 2.5) can be employed. The equations are as follows:

$$\Delta p = \Delta\rho + d\,\Delta\rho + \Delta d_{ion} + \Delta d_{trop} + \Delta\varepsilon(p) \qquad (2.18)$$

$$\Delta\Phi = \Delta\rho + d\,\Delta\rho + \lambda\,\Delta N - \Delta d_{ion} + \Delta d_{trop} + \Delta\varepsilon(\Phi) \qquad (2.19)$$

$$\Delta\dot{\Phi} = \Delta\dot{\rho} + \Delta\dot{d}\rho - \Delta\dot{d}_{ion} + \Delta\dot{d}_{trop} + \Delta\varepsilon(\dot{\Phi}) \qquad (2.20)$$

where $\Delta$ ... represents the double difference operator between two stations and two satellites.

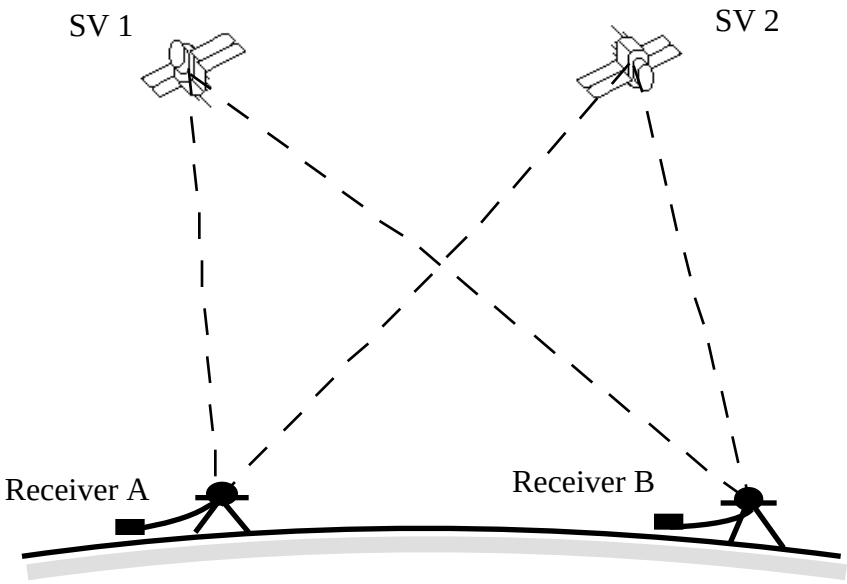


**Figure 2.5 Double Differencing Between Receivers and Satellites**

As shown equations (2.18) to (2.20), the double differenced observables have cancelled out both the receiver and satellite clock errors and have further reduced the orbital and propagation effects. In addition, this method allows to optimally exploit the integer nature of carrier phase ambiguity. In fact, double differencing GPS positioning technique is considered as the best processing method and is extensively used for GPS applications (Remondi, 1984, Cannon, 1987, 1991).

It is also noted that the double difference of carrier phase observation contains the double difference ambiguity term. In order to achieve high positioning accuracy, the integer ambiguity must be correctly resolved before the beginning of the mission and then fixed in kinematic surveys. In shipborne case, however, the ship can never be static even if anchored in the harhour. Cycle slips often occur in carrier phase observations due to ship dynamics and multipath effects. Therefore, it is necessary to resolve ambiguity on the fly for

precise GPS positioning in the marine environment. It is one of the main problems to be dealt with in this thesis.

CHAPTER 3

# POST-PROCESSING METHODOLOGY

In this chapter, two processing methods for kinematic GPS positioning are examined. One is the carrier phase smoothing of the code method. The other is the least-squares ambiguity search technique. At the end of this chapter, ambiguity resolution on the fly with a multi-receiver configuration is also discussed.

## 3.1 CARRIER PHASE SMOOTHING OF CODE

The carrier phase smoothing of the code combines pseudorange and carrier phase observations to form an instantaneous pseudorange measurement with much lower noise and multipath effects than the code measurement alone. This technique was first proposed by Hatch (1982) using carrier phase measurements to filter the pseudoranges. The method was thereafter enhanced by other investigators, e.g., Lachapelle et al (1987, 1989), Goad (1990), Cannon & Lachapelle (1992), to model or control ionospheric and multipath effects.

The general carrier phase smoothed pseudorange at time k may be written as (Lachapelle et al 1987):

$$\hat{P}_k = W_{P_k} P_K + W_{\Phi_k} \{ \hat{P}_{K-1} + ( \Phi_k - \Phi_{k-1} )\} \qquad (3.1)$$

$$W_{P_K} = W_{P_{K-1}} - 0.01 \qquad \{e.g.\ 0.01 \le W_{P_K} \le 1.00\} \qquad (3.2)$$

$$W_{\Phi_K} = W_{\Phi_{K-1}} - 0.01 \qquad \{e.g.\ 0.00 \le W_{\Phi_K} \le 0.99\} \qquad (3.3)$$

where $P_k$ ... is the measured pseudorange at $t_k$

$\Phi_k$ ... is the measured carrier phase measurement at $t_k$

$P_k$ ... is the "smoothed" measurement at $t_k$

At time $t_1$ ( first epoch):

$$P_1 = P_1 \qquad (3.4)$$

The improved ratio between raw and carrier phase smoothed pseudorange is estimated as (Goad, 1990):

$$\sigma(P_k) \,/\, \sigma(P_k) \quad 1.5 - 3 \qquad (3.5)$$

Since the effect of ionosphere on code has the opposite sign than the effect on the carrier phase, two smoothing ramp methods can be implemented in parallel to reduce the ionospheric error (Cannon & Lachapelle, 1991). These two ramps are N/2 epochs apart (e.g., 100 is number of measurements in this example). Each ramp is reset at every N epochs. The notion of two parallel carrier phase smoothing is shown in Figure 3.1 .

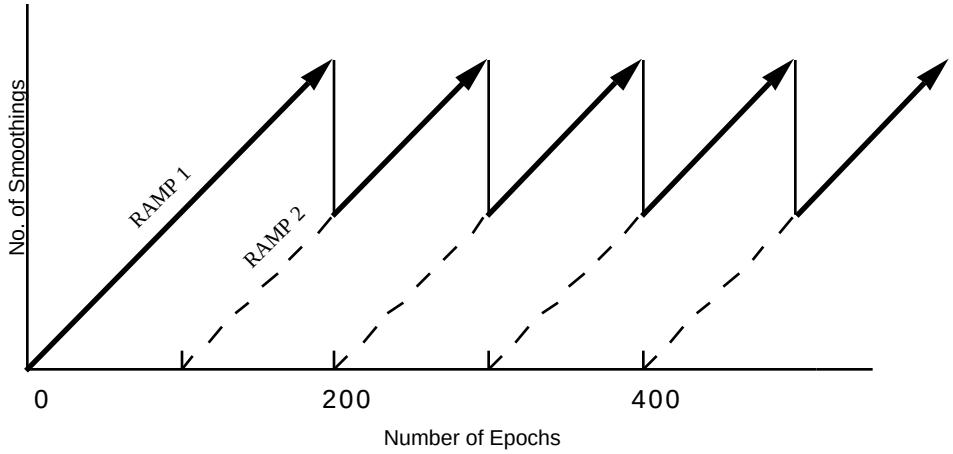


**Figure 3.1: "Dual Ramp" Carrier Phase Smoothing**

Initially and after cycle slips, these two ramps are initialized at the same time. After N/2 epochs, the first filter is reset and the second filter is used for N/2 more epochs. By this time, the second ramp is reset and the smoothing continues with the first ramp again.

Carrier phase smoothed code has reached accuracies at the 25 - 100 cm level in land kinematic mode using narrow correlator spacing technology (Cannon & Lachapelle, 1992). In the marine environment, an accuracy of the 50 - 100 cm level is achieved (shown in the following Chapter). Therefore, when the correct ambiguity cannot be solved due to a variety of factors, the use of carrier phase smoothed code method is preferable.

## 3.2 LEAST-SQUARES AMBIGUITY SEARCH TECHNIQUE

The least-squares ambiguity search technique with the use of primary and secondary satellites was proposed by Hatch (1991) and a modified version was developed by Lachapelle et al (1992).

The least-squares ambiguity search approach can be conducted through three steps: an approximate position is estimated, an entire set of four primary satellites ambiguities centered on the initial position are generated and a least-squares search technique is applied to identify the correct integer ambiguity combination. The centre of the search space can be estimated by using a double difference code solution or carrier phase smoothed code solution. The size of the search cube depends on the accuracy of the approximate solution. Generally, the search volume is bounded by

$$x = x_0 \pm k\,\sigma_{x0} \tag{3.6}$$

$$y = y_0 \pm k\,\sigma_{y0} \tag{3.7}$$

$$z = z_0 \pm k\,\sigma_{z0} \tag{3.8}$$

where $x_0, y_0, z_0$ are the coordinate estimates from a code or carrier phase smoothed code solution; $\sigma_{x0}$, $\sigma_{y0}$, $\sigma_{z0}$ are their standard deviations. The constant k can be set to 3 or 4, which corresponds to a confidence level of more than 99%. It is required that the initial coordinates should be determined as accurately as possible since the search space defined by the above error bounds must include the correct but yet unknown solution corresponding to the correct ambiguity set. If the search space is larger, the number of potential ambiguity solutions will increase , and more computation time will be required.

The least-squares ambiguity search technique exploits the fact that only three of the double difference phase ambiguities are independent. Once the double difference phase ambiguities are known, the position of the moving receiver can be determined, and the ambiguities corresponding to remaining satellites can be fixed. Four primary satellites are required to generate an entire set of ambiguities. In the three - dimensional cube, the ambiguities are calculated for the eight corners of the block for the three double difference pairs. The maximum and minimum ambiguities for each double difference pair are saved. Combinations of potential ambiguities can be generated using nest increment loops between the minimum and maximum of each ambiguity. The total number of potential ambiguity sets for double difference pairs of four primary satellites are

$$\text{Nbr of sets} = \prod_{i=1}^{3} [(\text{max. ambiguity} - \text{min. ambiguity}) + 1]_i \qquad (3.9)$$

Based on the potential ambiguity combinations, the potential solution of the moving receiver can be uniquely determined, then the ambiguities of the remaining secondary satellites can be computed as follows:

$$\Delta N_s ( j ) = \text{nint } (\textbf{Error!}) \qquad (3.10)$$

where $\Delta N_s (j)$ ... is the calculated ambiguity corresponding to the secondary satellite j.

$\Delta \Phi_{obs}(j)$ ... is the double difference phase observations in length units.

$\Delta\Phi_{calc}(j)$ ... is the double difference calculated ranges using satellite position and the potential solution.

$\lambda$ ... is the carrier phase signal wavelength.

nint(·) ... denotes the rounding of the value to the nearest integer number.

When the integer ambiguities have been determined, the measurement residuals can be calculated as

$$v(i) = \Delta\Phi_{obs}(i) - \Delta\Phi_{calc}(i) - \Delta N(i) \qquad (3.11)$$

where v (i) ... is the residual vector of phase observations for the primary and secondary satellites

Once the measurement residuals have been computed, the estimated variance factor can be estimated as:

**Error!**= **Error!** (3.12)

where **Error!** ... is the estimated variance factor

$C^{-1}$ ... is the covariance matrix of the carrier phase observation

ns ... is the number of satellites

At the correct potential solution, the calculated phase observations should be very close to the associated measured carrier phase observations and the residuals should be minimum. It would result in that the estimated variance factor should also be a minimum. For each potential ambiguity combination, the

estimated variance factor **Error!**is compared to a predetermined threshold applying the chi-squares statistical testing. If the estimated factor for a particular potential solution is less than the priori variance factor , this integer ambiguity combination is retained and further tested at the subsequent epochs. If the test fails, the potential integer ambiguity combination is rejected.

The variance factor statistic test corresponding to a single epoch observation is referred to as the local variance factor test, while the variance factor calculated using multiple epochs of observations is considered as a global variance factor. Usually, the number of satellites in view is less than eight. The degree of freedom of the local variance factor is therefore not greater than four. In the sense of statistical testing, the calculated variance factor is unstable due to the low number of redundant observations. It implies that the estimated local variance factor may vary a lot from one kinematic epoch to the subsequent epoch owing to receiver noise and environmental changes. For global variance factor testing, the degree of freedom is higher and the global estimated variance factor is more stable than the local estimated variance factor. Hence, in the statistical testing, a relatively loose threshold is employed for the local variance factor testing and a more stringent threshold is assigned to the global variance testing.

If more than one potential solution passes the statistical test at a given epoch, the ambiguity sets related to these potential solutions are saved and further examined at the subsequent epoch. If no potential solution passes the test, the whole least-squares ambiguity search process restarts at a new epoch. This process also restarts when cycle slips occur on the primary satellites during the search period.

When the number of potential solutions is reduced to a relatively low number (usually, 10 is used) after a certain number of tests, the smallest variance factor is compared with the second smallest variance factor to accelerate the convergence time of this search procedure. If the ratio is greater than a specified threshold (herein, 2 is chosen), the potential solution with the smaller variance is accepted as the correct ambiguity combination.

If dual frequency measurements are available, the widelane methods can be used. The widelane carrier phase observations are constructed from L1 and L2 carrier phase observations as follows:

$$\varphi_\Delta = \varphi_1 - \varphi_2 \tag{3.13}$$

with

$$f_\Delta = f_1 - f_2; \quad \lambda_\Delta = c / f_\Delta = 86.25 \text{ cm} \tag{3.14}$$

The wavelength is increased to some 86 cm (compared to 19 cm for L1 or 24 cm for L2), which makes it more easy to estimate the corresponding ambiguities. However, if only single frequency data is available, the use of a multi-receiver configuration for ambiguity resolution on the fly might be improved.

## 3.3 AMBIGUITY RESOLUTION ON THE FLY WITH A MUTI-RECEIVER CONFIGURATION

The use of a multi-receiver configuration, such as a triple receiver system (two monitors and one remote, or one monitor and two remotes) or a quadruple

receiver system (two monitors and two remotes), might improve the convergence time for least-squares ambiguity resolution with single frequency data. There are four main advantages of using such a multi-receiver system for on-the-fly ambiguity resolution. The first one is that one can estimate more reliably the bias effects of receiver noise and carrier phase multipath and can average out these biases more effectively with a multi-receiver system than with a single monitor - remote pair. The second advantage is that the size of the initial ambiguity search space can be reduced since the approximate position of the moving receiver can be determined with a higher level of accuracy. The third advantage is that the double difference integer ambiguities between two monitor and two remote receiver pairs can be resolved quickly since the separation between these units is short (a few of metres) and easily determined. The fourth advantage is that the double difference ambiguities among the various monitor - remote receiver pairs satisfy certain relationships which can be used as constraints to speed up the ambiguity search process and to increase its reliability.

This novel concept was first developed and implemented by Lachapelle et al (1993c). The results of the quadruple receiver system for ambiguity resolution on the fly are also addressed in Chapter 5 in this thesis. In the following, the relationships of the double difference ambiguities among the various monitor-remote receiver pairs are derived.

In order to derive the relationship between the double difference integer ambiguities, one triple receiver system (one monitor and two remotes) is considered. The subscript $0$ is used to represent the monitor receiver and subscripts $1, 2$ denote remote receivers. Regardless of the effects of biases in

Eqn. (2.19), the double difference carrier phase measurement equation can be written as:

$$\begin{aligned}\Delta\Phi_{1-0} &= [(\Phi_1^j - \Phi_1^i) - (\Phi_0^j - \Phi_0^i)] \\ &= [(\rho_1^j - \rho_1^i) - (\rho_0^j - \rho_0^i)] - \lambda[(N_1^j - N_1^i) - (N_0^j - N_0^i)] \\ &= \Delta\rho_{1-0} + \lambda \Delta N_{1-0} \end{aligned} \quad (3.15)$$

$$\begin{aligned}\Delta\Phi_{2-0} &= [(\Phi_2^j - \Phi_2^i) - (\Phi_0^j - \Phi_0^i)] \\ &= [(\rho_2^j - \rho_2^i) - (\rho_0^j - \rho_0^i)] - \lambda[(N_2^j - N_2^i) - (N_0^j - N_0^i)] \\ &= \Delta\rho_{2-0} + \lambda \Delta N_{2-0} \end{aligned} \quad (3.16)$$

where the superscripts *i* and *j* represent the satellites. The superscript *i* is considered the base satellite. Subtracting Eqn. (3.15) from (3.16), the double difference carrier phase measurement between two remote receivers is:

$$\begin{aligned}\Delta\Phi_{2-1} &= [(\Phi_2^j - \Phi_2^i) - (\Phi_1^j - \Phi_1^i)] \\ &= [(\rho_2^j - \rho_2^i) - (\rho_1^j - \rho_1^i)] - \lambda[(N_2^j - N_2^i) - (N_1^j - N_1^i)] \\ &= \Delta\rho_{2-1} + \lambda \Delta N_{2-1} \end{aligned} \quad (3.17)$$

In simplified form, Eqn. (3.17) can be written as:

$$\Delta N_{2-1} = \Delta N_{2-0} - \Delta N_{1-0} \quad (3.18)$$

Since the distance between two remote receivers on the moving platform is short, the double difference ambiguity $\Delta N_{2-1}$ can be determined quickly and reliably. It can thereafter be used as a constraint in solving the double difference integer ambiguities between the monitor and remote receivers ( $\Delta N_{1-0}$

$\Delta N_{2-0}$). If the more satellites are available and more receivers, such as a quadruple receiver system, are used, additional double difference ambiguity equations may be generated. If the double difference ambiguity relations among these units are introduced as additional constraints to isolate the correct integer ambiguity set, it improves the convergence time for the ambiguity search process.

CHAPTER 4

# SHIPBORNE TESTING AND RESULTS USING P CODE AND HIGH PERFORMANCE C/A CODE TECHNOLOGIES

In order to assess and compare two the processing methods discussed in Chapter 3, namely carrier phase ambiguity resolution on the fly and carrier phase smoothing of the code, a detailed analysis of a survey launch test is described. This chapter describes the field test conducted, analyses the code multipath and ionospheric effects, and assesses and compares the performance of ambiguity resolution on the fly for two receiver technologies. They are narrow correlator spacing single frequency C/A code and dual frequency P code technologies. The achievable accuracy of the carrier phase solution, code solution and carrier phase smoothed code solution are also discussed. The results described herein were reported by Lachapelle et al (1993b).

## 4.1 DESCRIPTION OF DATA SETS

A marine survey launch test was conducted by The University of Calgary and the Canadian Hydrographic Service (CHS) in early September 1992 off the

cost of Sidney, B.C.. The GPS observations selected for post-processing in this thesis were collected on September 3 over a period of 40 minutes. The survey launch trajectory for the selected data is shown in Figure 4.1. The boat traveled at cruising speeds of 10 to 15 knots (18 to 27 km $h^{-1}$). The satellites observed, together with their azimuths and elevations during the period of the selected data, are listed in Table 4.1. The PDOP varied from 1.9 to 2.6. The differential mode was employed and one GPSCard™ and one P-XII unit were used on-shore. The distance between these two shore-based monitor stations was 2.6 m. The distance between the shore units and the launch ranged from 10 to 24 km.

The antenna configuration used on the launch is shown in Figure 4.2. Three GPScard™s and one P-XII unit were used. All code and carrier phase data were recorded at a data rate of two Hz using PC laptops. The three-GPSCard™ configuration was used to obtain redundant observations for the on-the-fly ambiguity resolution solutions and to estimate the attitude parameters of the launch. The results of the attitude parameter estimation experiment are reported by Lu et al (1993). The distances between the three GPSCard™ units were measured with an accuracy of about one cm, as shown in Figure 4.2. These distances will be used later to independently check the double difference carrier phase ambiguities estimated between the shore antenna and each one of the three launch-based GPSCard™ antennas.

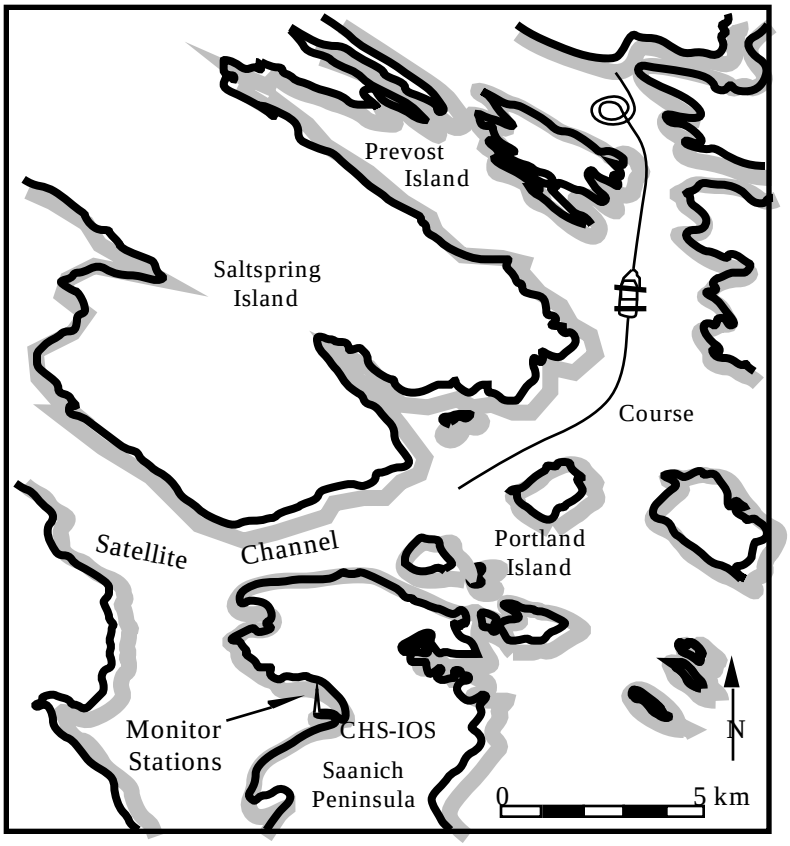


**Figure 4.1: Launch Trajectory Observed for Marine Test**

**Table 4.1: SV Observed and their Azimuth and Elevation**

| SV | Azimuth | Elevation |
|---|---|---|
| 03 | 130 - 143˚ | 40 - 22˚ |
| 17 | 68 - 92˚ | 71 - 55˚ |
| 21 | 225 - 235˚ | 31 - 48˚ |
| 23 | 204 - 108˚ | 71 - 86˚ |
| 26 | 67 - 50˚ | 35 - 28˚ |
| 28 | 308 - 295˚ | 34 - 48˚ |
| PDOP = 2.6 - 1.9 | | |

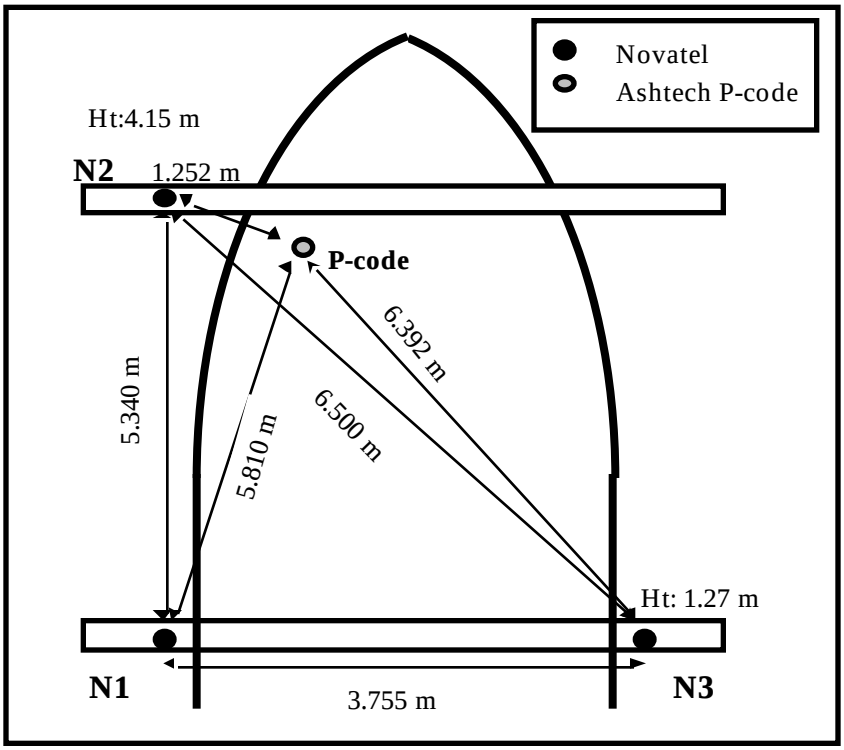


**Figure 4.2: GPS Antenna Configuration on Launch**

All shore and launch-based P-XII and GPSCard™ antennas were equipped with chokering groundplanes except one GPScard™ antenna (No.2) on the survey launch. The use of such groundplanes is to minimize multipath effects and to compare convergence time for ambiguity resolution on the fly with antenna No. 2 which had no chokering ground planes.

In order to analyze the effect of Selective Availability during the test, the single point positioning of the monitor station data (Novatel GPSCard™) is examined. The sample single point positioning residuals for SV21, SV23 are shown in Figures 4.3 and 4.4 respectively. From these figures, it is seen that Selective Availability is minimal during the test. To further evaluate the quality of the data, the multipath and ionospheric effects are discussed in the following section.

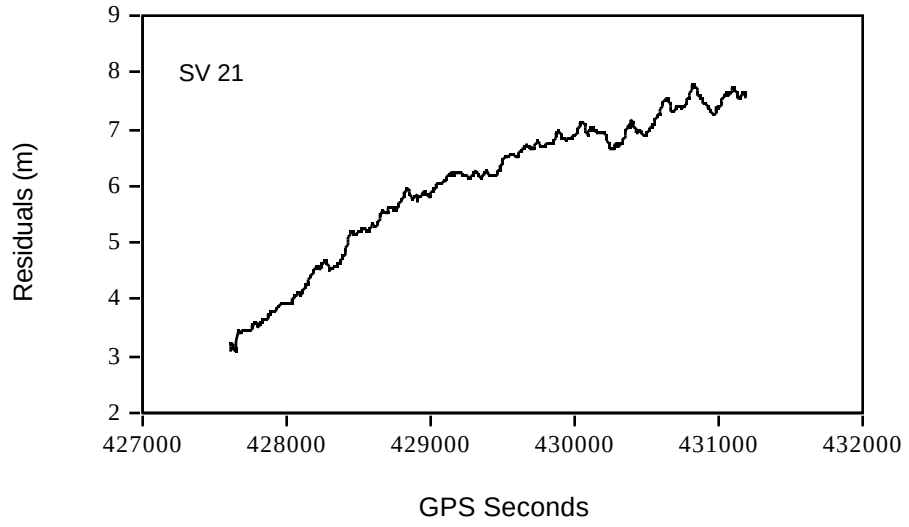


**Figure 4.3: Residuals for Single Point Positioning on Satellite 21**

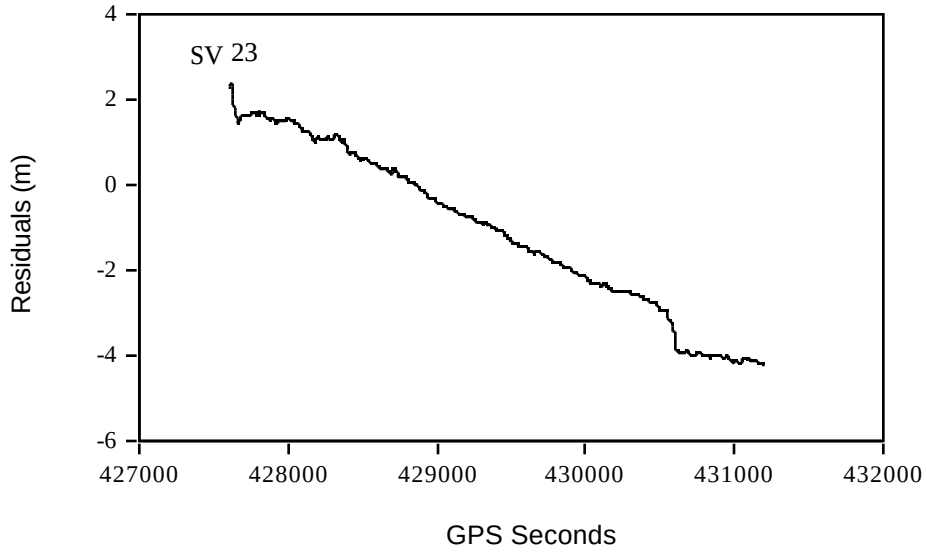


**Figure 4.4: Residuals for Single Point Positioning on Satellite 23**

## 4.2 Multipath and Ionospheric Effects

An estimate of the combined effect of code noise and multipath is given as (Lachapelle, 1991a):

$$\delta = \Delta P - ( \Delta \Phi + \Delta N) \qquad (4.1)$$

Since carrier phase measurements are usually two order of magnitude less noisy than code measurements, the difference between code and carrier phase observations is considered as being mostly due to receiver code noise and multipath errors.

Tables 4.3, 4.4 and 4.5 give statistics between double difference code and carrier phase measurements. These are results between the shore receiver, which was fitted with a chokering and three launch receivers, two of which were fitted with a chokering and the third one not. The rms values are similar for the three pairs of receivers and appear to make little differences on receiver code noise and multipath. It shall be shown in a later section, however, that the chokerings are effective in reducing carrier phase multipath. If one divides the rms values given in Tables 4.3, 4.4 and 4.5 by $\sqrt{2}$, one obtains the combined effect of code noise and multipath on a single code measurement. The effect ranges from 22 to 68 cm and agrees well with the estimated values in (Lachapelle et al, 1993a). Similar results are obtained with P-XII PL1 and PL2 data. The P-XII C/A code results are substantially higher, as expected.

**Table 4.2: Multipath Effects For GPScard™ Antenna 1 (With Chokering)**

| SV (Base SV: 23) | Δ Code minus Δ Carrier (m) | | | |
|---|---|---|---|---|
| | Max. | Min. | Mean | RMS |
| 03 | 1.48 | -1.14 | 0.25 | 0.58 |
| 17 | 1.16 | -0.29 | 0.49 | 0.58 |
| 21 | 1.01 | -2.28 | -0.35 | 0.58 |
| 26 | 3.14 | -1.16 | 0.89 | 1.15 |
| 28 | 1.43 | -0.91 | 0.21 | 0.47 |

**Table 4.3: Multipath Effects For GPScard™ Antenna 2 (Without Chokering)**

| SV (Base SV: 23) | Δ Code minus Δ Carrier (m) | | | |
|---|---|---|---|---|
| | Max. | Min. | Mean | RMS |
| 03 | 2.07 | -0.78 | 0.55 | 0.70 |
| 17 | 1.34 | -0.39 | 0.53 | 0.62 |
| 21 | 1.08 | -1.55 | -0.05 | 0.43 |
| 26 | 2.81 | -0.93 | 0.87 | 1.11 |
| 28 | 1.48 | -1.16 | 0.37 | 0.51 |

**Table 4.4: Multipath Effects For GPScard™ Antenna 3 (With Chokering)**

| SV (Base SV: 23) | Δ Code minus Δ Carrier (m) | | | |
|---|---|---|---|---|
| | Max. | Min. | Mean | RMS |
| 03 | 1.92 | -1.57 | 0.38 | 0.64 |
| 17 | 1.57 | -0.22 | 0.57 | 0.63 |
| 21 | 0.89 | -1.73 | -0.17 | 0.47 |
| 26 | 3.01 | -0.96 | 0.81 | 1.06 |
| 28 | 1.32 | -0.85 | 0.24 | 0.43 |

The ionospheric corrections on code and carrier phase measurements can be calculated by Eqns. (2.12) and (2.13). The total ionospheric phase delay at an epoch can not be estimated since the phase ambiguities N (L1) and N(L2) cause some difficulty in determining the value. If both L1 and L2 carrier phase are continuously tracked, i.e, there is no cycle slip during the interval ($t_1$ , $t_2$), the differential ionospheric delay over ($t_1$ , $t_2$) can be computed.

Figure 4.5 shows the ionospheric delay on P(L1) for satellite 23 on the survey launch. Figures 4.6 and 4.7 gives the differential ionospheric delays for satellite 23 on L1 (C/A) carrier phase and L1 (P1) carrier phase respectively. Although the corrections from Figures 4.6 and 4.7 have same shape, the differential ionospheric delay on L1 (C/A) carrier phase ranges within 3 centimetres. The differential ionospheric delays on L1 (P1) carrier phase, however, drifts with time. Similar performance is obtained with other satellites.

The difference of ionospheric delays between L1 (C / A) and L1 (P1) carrier phase may be caused by Ashtech P-XII receiver problems.

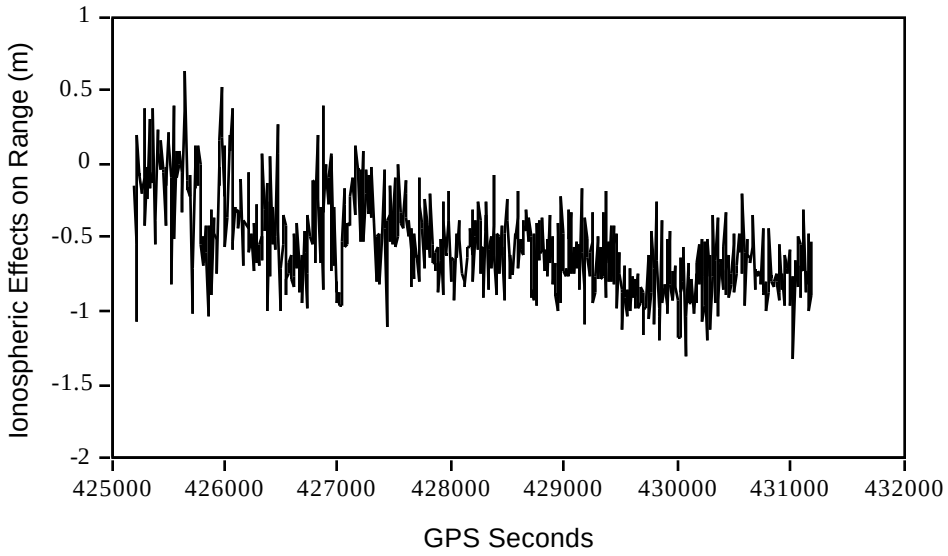


**Figure 4.6: The Ionospheric Delay on Range for Satellite 23**

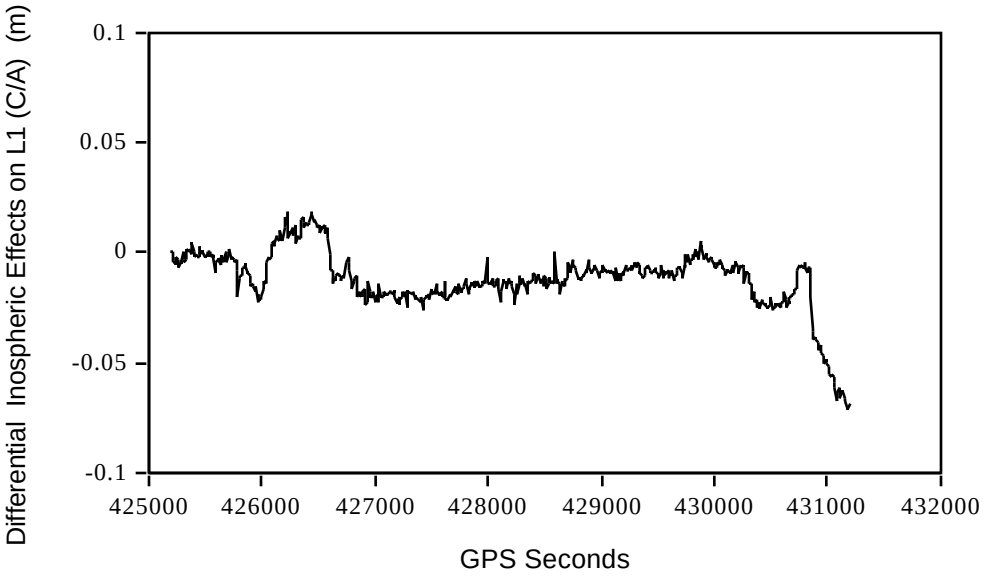


**Figure 4.6: The Differential Ionospheric Delay on L1(C/A) Carrier Phase for Satellite 23**

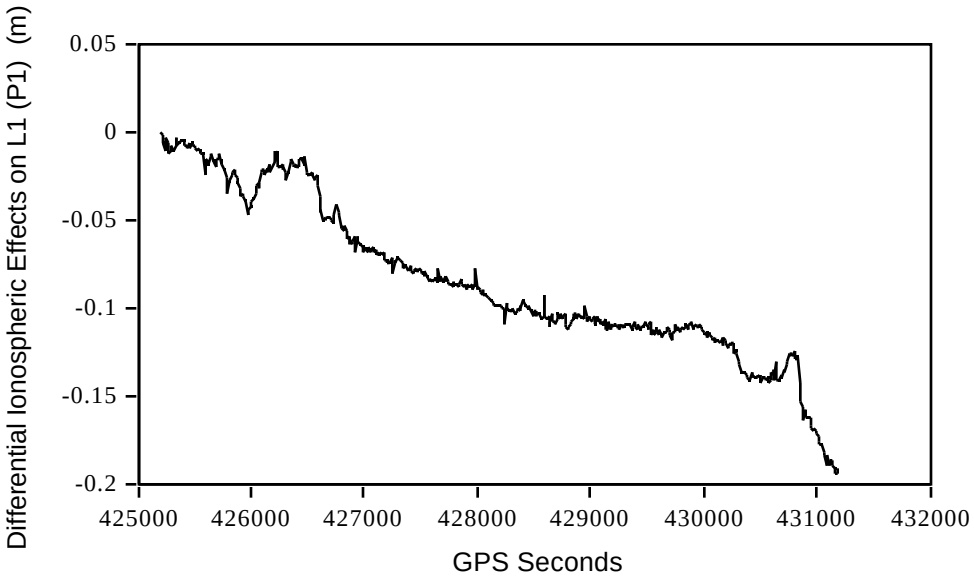


**Figure 4.7: The Differential Ionospheric Delay on L1(P1) Carrier Phase for Satellite 23**

## 4.3 Ambiguity Resolution on the Fly for Ashtech P-XII Reciver

The least-squares ambiguity search technique described in Chapter 3 is tested using Ashtech P-XII receiver shipborne measurements. In order to obtain several solutions for the carrier phase ambiguities and therefore improve reliability, several trials were conducted using a different starting point, shifted 20 seconds forward from the previous one. This 20-second shift is sufficient to decorrelate code and carrier receiver noise at both the monitor and the launch and to decorrelate multipath at the launch. Several quasi-independent solutions are thus obtained for the ambiguities. Software FLYKIN™ (Lachapelle et al, 1992) was used for this purpose. A priori carrier phase variance $\sigma_{\Delta\varphi}$, the number of trials, number of count ambiguity solutions, success rate (number of trials / number of identical solutions) and average observation period required for each type of solutions are given in Table 4.5.

**Table 4.5: Ambiguity Resolution on the Fly -Performance Statistics (Ashtech P-XII Receiver)**

| Receiver and Observation Type | $\sigma_{\Delta\varphi}$ | Nbr of trials | Nbr of Correct Trials | Success rate | Average Period Required |
|---|---|---|---|---|---|
| P-XII (Chokerings) | | | | | |
| P1 and Φ | 15 mm | 10 | 10 | 100% | 865 |
| P2 and Φ | 15 mm | 29 | 27 | 93% | 545 |
| Widelane (L1-L2) | 20 mm | 58 | 40 | 69% | 2 |

The success rate is 100% for the P-XII L1, 93% for L2 and 69% for widelane (L1-L2) cases. In the L2 case, a 100% success rate could have been obtained by increasing the *a priori* carrier phase standard deviation $\sigma_{\Delta\varphi}$ This would have increased the period required for ambiguity resolution. In the widelane case, 69% of the solutions yielded identical sets of ambiguities. The remaining 31% produced different solutions. These incorrect solutions were often off by one cycle and this is due to a combination of the effects of multipath and satellite geometry. The time to convergence for the widelane case is very short, namely a few seconds. This is due to the favourable ratio between the carrier phase noise and the 86 cm wavelength of the widelane carrier.

In order to independently verify that the P-XII L1, L2 and L1-L2 ambiguity solutions which are statistically identified as the correct ones are indeed correct, the following equation is used to test the double difference ambiguities obtained on L1, L2 and L1-L2 for each pair of satellites:

$$\Delta N_{L1-L2} = \Delta N_{L1} - \Delta N_{L2} \qquad (4.2)$$

where $\Delta N_{L1-L2}$ is the double difference ambiguity of the L1-L2 observations and $\Delta N_{L1}$ and $\Delta N_{L2}$, the corresponding ambiguities on L1 and L2, respectively. The double difference ambiguities for L1, L2 and the widelane carrier phase are listed in Table 4.6. In each case, the equation was satisfied, which confirmed that all ambiguities were correctly identified.

**Table 4.6: Double Difference Ambiguities for L1, L2 and Widelane (L1-L2) Carrier Phase (Base Sat. 23)**

| Sv No. | Δ N1 | Δ N2 | Δ N1−2 |
|---|---|---|---|
| Sv 03 | 21315295.0 | -2383032.0 | 23698327.0 |
| Sv 28 | -2490925.0 | 577601.0 | -3069526.0 |
| Sv 26 | -4576228.0 | -9749140.0 | 5172912.0 |
| Sv 21 | -903911.0 | 1051151.0 | -1955062.0 |
| Sv 17 | -1813835.0 | -1484608.0 | -329227.0 |

Sample double difference carrier phase residuals obtained after integer ambiguity resolution are shown in Figure 4.8 to 4.10 for P-XII L1, L2 and widelane (L1-L2) data, respectively. A comparison of the *a posteriori* rms residuals with the *a priori* standard deviations given in Table 4.5 shows that the latter have the correct order of magnitude, once a safety factor of 2 is applied to increase the success rate. Figures 4.8 and 4.9 clearly indicate the presence of carrier phase multipath and a strong correlation between the double difference residuals of P-XII L1 and L2 data. The widelane data tends to have a larger noise effect.

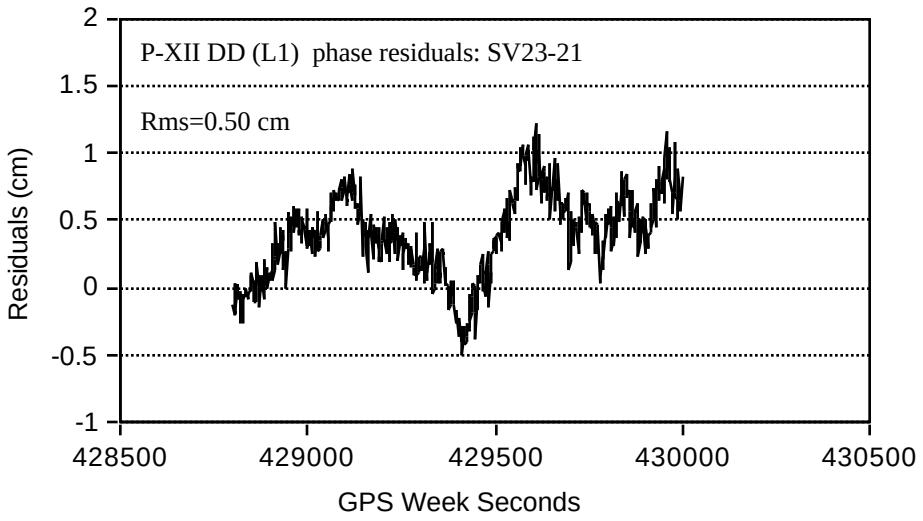


**Figure 4.8: P-XII L1 Double Difference Carrier Phase Residuals for SV 23-21**

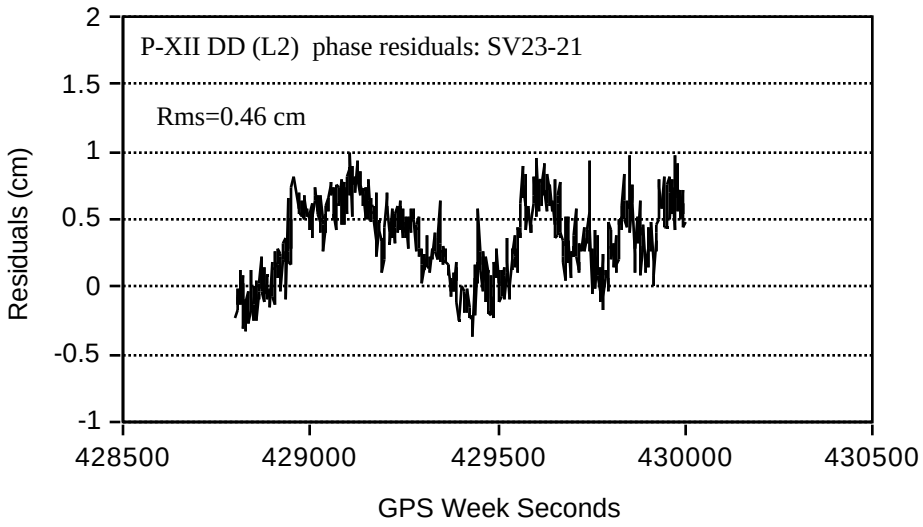


**Figure 4.9: P-XII L2 Double Difference Carrier Phase Residuals for SV 23-21**

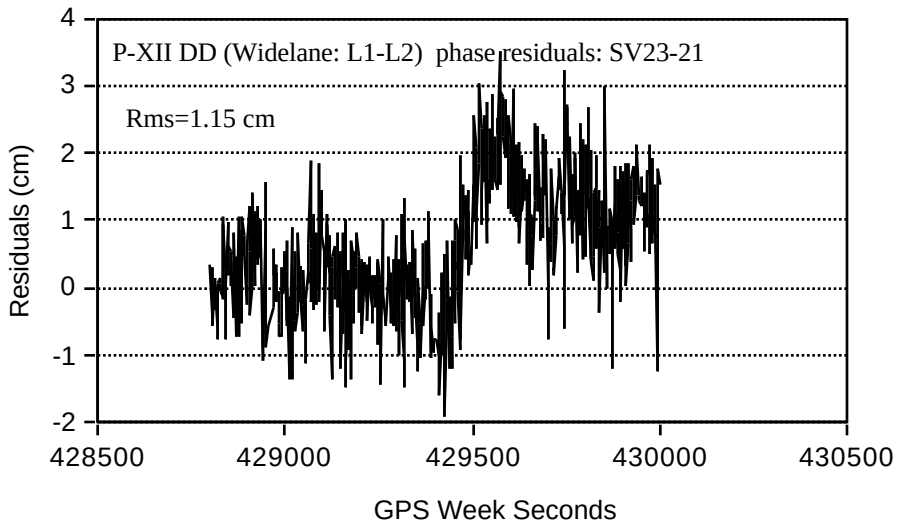


**Figure 4.10: P-XII Widelane (L1-L2) Double Difference Carrier Phase Residuals for SV 23-21**

## 4.4 Ambiguity Resolution on the Fly for NovAtel Narrow Correlator Spacing C/A Code Receiver

Ambiguity Resolution on the fly with the narrow correlator spacing C/A code receiver (Novatel GPSCard™) data on the survey launch is also successfully achieved. Tables 4.7 to 4.9 show results of the ambiguity resolution for GPSCard™ No.1 to No.3, respectively. From these tables, ambiguity resolution for the total of 23 trials (9 trials for GPSCard™ No.1, 7 trials for GPSCard™ No.2, 7 trials for GPSCard™ No.3) is correctly obtained. Such a high success rate is achieved by increasing the *a priori* standard deviation of the double difference carrier phase measurements (e.g. Lachapelle et al 1993a). The average time required using the GPSCard™ with no chokering groundplane on the launch increases by some 60%. The reason is that the use of chokerings does reduce

carrier phase multipath substantially, a fact which was not evident from Table 4.2 and 4.4.

**Table 4.7: Performance Statistics of Ambiguity Resolution on the Fly Using Novatel GPSCard™ No.1 Data (With Choke Ring)**

| Sv No. | Δ N (Base Sat. 23) | |
|---|---|---|
| Sv 03 | 11030055.0 | No. of trials: 9 |
| Sv 28 | -1575353.0 | No. of correct trials: 9 |
| Sv 26 | 4726106.0 | Success rate: 100% |
| Sv 21 | -1575477.0 | Average epochs required: 1032s |
| Sv 17 | 6301618.0 | Standard phase variance: 18mm. |

**Table 4.8: Performance Statistics of Ambiguity Resolution on the Fly Using GPSCard™ No.2 Data (Without Choke Ring)**

| Sv No. | Δ N (Base Sat. 23) | |
|---|---|---|
| Sv 03 | 17329679.0 | No. of trials: 7 |
| Sv 28 | -3150685.0 | No. of correct trials: 7 |
| Sv 26 | 9452490.0 | Success rate: 100% |
| Sv 21 | 1575358.0 | Average epochs required: 1825s |
| Sv 17 | 11027895.0 | Standard phase variance: 18mm. |

**Table 4.9: Performance Statistics of Ambiguity Resolution on the Fly Using Novatel GPSCard™ No.3 Data (With Choke Ring)**

| Sv No. | Δ N (Base Sat. 23) | |
|---|---|---|
| Sv 03 | 4726255.0 | No. of trials: 7 |
| Sv 28 | -1575392.0 | No. of correct trials: 7 |
| Sv 26 | 3150698.0 | Success rate: 100% |
| Sv 21 | -1575558.0 | Average epochs required: 1146s |
| Sv 17 | 3150816.0 | Standard phase variance: 18mm. |

The higher multipath influence on the GPSCard™ with no chokering is also seen from the double difference carrier phase residuals. Shown in Figures 4.11 and 4.12 are the SVs 23-21 carrier phase double difference residuals with fixed integer ambiguities for two GPScard™ s, one with chokering groundplanes at both the monitor and the launch and another with a chokering at the monitor only. It is evident that the residuals for the GPSCard™ with a chokering on the launch are substantially lower than those obtained for GPSCard™ with no chokering on the launch. The time period required for ambiguity resolution is a little longer in this case. The two likely reasons are (i) larger carrier phase multipath and (ii) much longer monitor-mobile distances, namely 10 - 24 km.

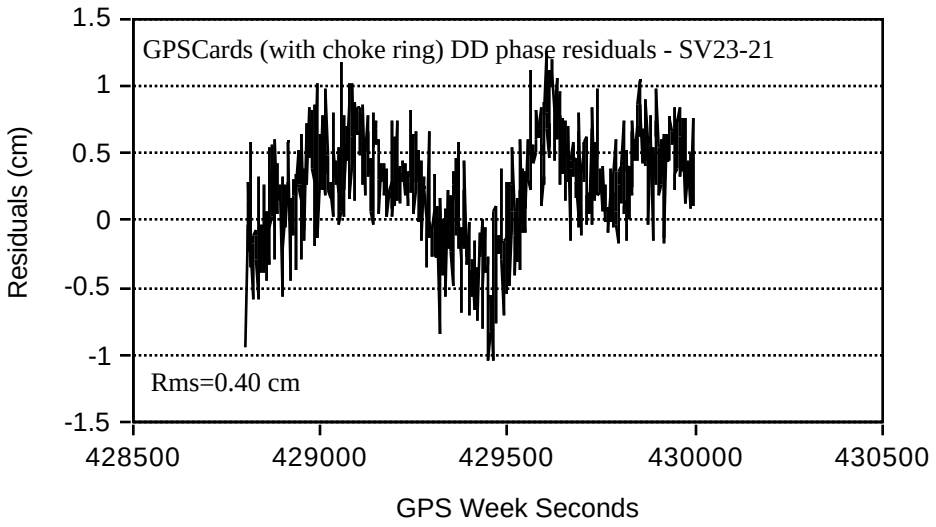


**Figure 4.11: GPSCard™ Double Difference Carrier Phase Residuals for SV 23-21 (Chokering Groundplanes at both the Monitor and Launch)**

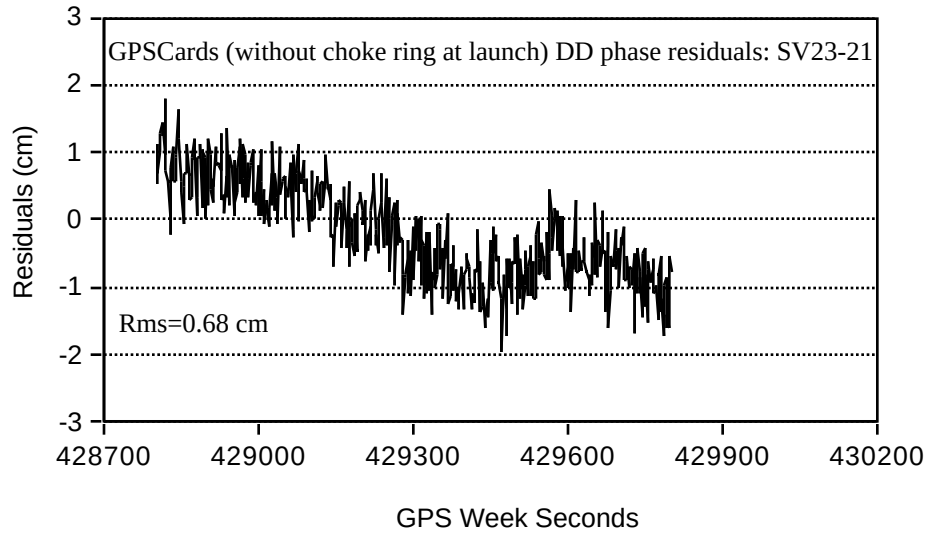


**Figure 4.12: GPSCard™ Double Difference Carrier Phase Residuals for SV 23-21 (Chokering Groundplanes at the Monitor only)**

The correctness of the ambiguity solutions is verified by a similar method as discussed previously. For any two GPSCard™ units i and j on the launch and the monitor unit k, the following double difference ambiguity relation can be derived:

$$\Delta N_{i-j} = \Delta N_{i-k} - \Delta N_{j-k} \quad (4.3)$$

Since the distances between the antennas on the launch are short and known, the double difference ambiguities between these can be determined reliably in a few seconds of observations (e.g., Cannon et al, 1992c) In each case, the equation was satisfied, which confirmed that all single frequency GPSCard™ ambiguities are also correctly identified.

Equation 4.3 cannot only be used to verify the ambiguity solutions, but also can be used as a constraint to speed up the ambiguity search process and to increase the reliability of the process. This will be addressed in Chapter 5.

## 4.6 Carrier, Code and Carrier Phase Smoothing of Code Solutions

In order to illustrate the level of accuracy achieved for the launch track with fixed ambiguities, the carrier phase solutions are evaluated by (i) trajectory comparisons between any two of three kinds of carrier phase L1, L2 and widelane (L1-L2) for Ashtech P-XII receiver, (ii) the distance comparisons between any two of the three GPSCard™ units calculated at each epoch using the fixed ambiguity solutions and the corresponding measured distances shown in Figure 4.2.

The trajectory differences in latitude, longitude and height components obtained with the fixed ambiguity solutions for carrier phase L1 and L2, and L1 and widelane (L1-L2) are presented in Figures 4.13 and 4.14. Comparing Figure 4.13 with Figure 4.14, the solution differences between carrier phase L1 and L2 are smaller than those obtained between carrier phase L1 and widelane (L1-L2). The reason is that widelane (L1-L2) modify the errors, such as ionospheric effect,

multipath and observation noise (Abidin, 1992). Reviewing the rms from these graphs, it is noted that the accuracy of the height component is the weakest and the longitude component is the strongest. This is consistent with general GPS solutions, as expected and is dependent on satellite geometry.

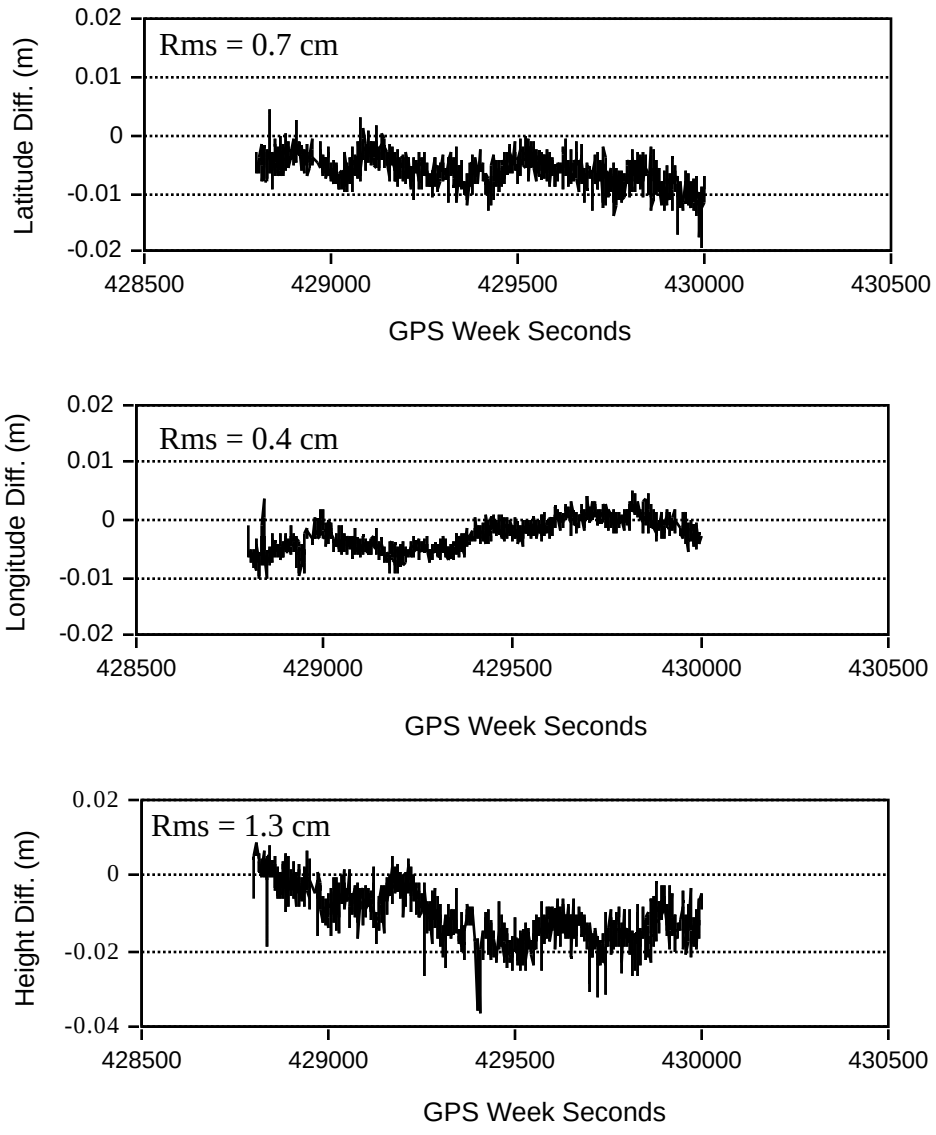


**Figure 4.13: Solution Difference Between L1 and L2 Carrier Phase with Fixed Ambiguity.**

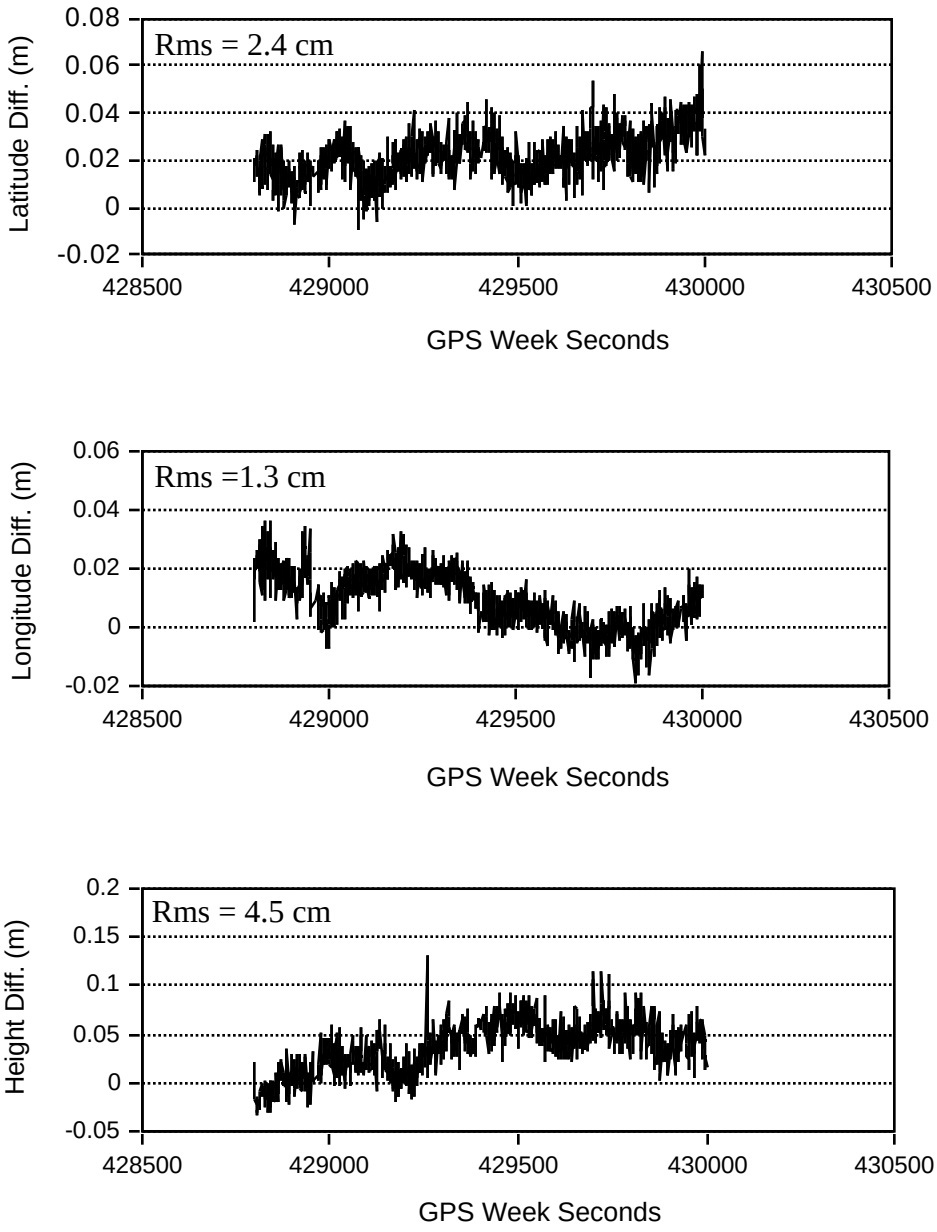


**Figure 4.14: Solution Difference Between L1 and Widelane (L1-L2) Carrier Phase with Fixed Ambiguity.**

The differences between the measured and calculated distances are shown in Figure 4.15 and 4.16 for the GPSCard™ units 1 and 2, and 1 and 3, respectively. The rms differences are 1.5 and 0.5 cm, respectively. The smaller value in the latter case is due to the fact that chokering groundplanes are used

both at the monitor and on the launch. These values are indicative of the level of positioning accuracy achievable using fixed ambiguities determined to their correct integer values.

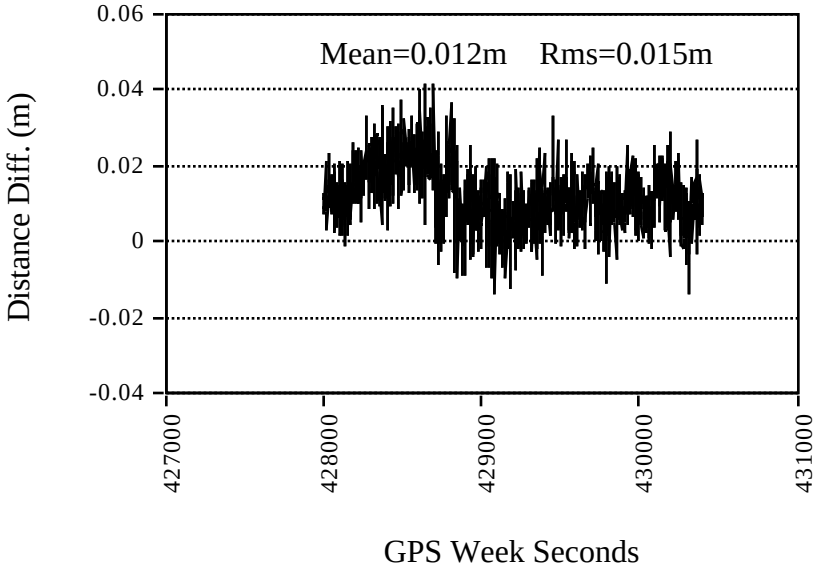


**Figure 15: Distance Calculated Using Fixed Ambiguity Solutions Minus Measured Distance Between GPSCard™ 1 and 2 on Launch**

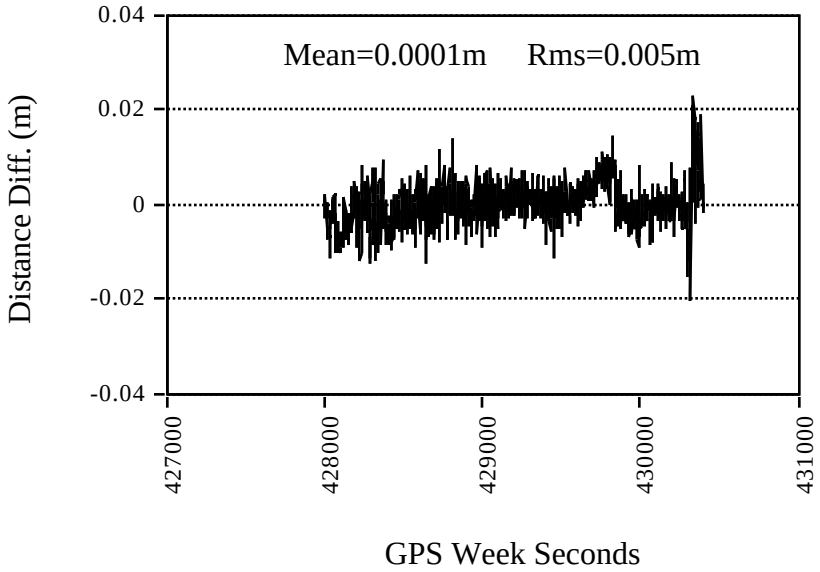


**Figure 4.16: Distance Calculated Using Fixed Ambiguity Solutions Minus Measured Distance Between GPSCard™ 1 and 3 on Launch**

Since the presence of multipath around a survey launch operating at sea is typically greater than multipath in the land kinematic environment, ambiguity resolution on the fly is more difficult to achieve reliably in the marine case than in the land case (e.g., Lachapelle et al, 1993a). In such a case, the use of a less accurate carrier phase smoothing of the code approach might be preferable.

The kinematic positioning performance of the two receiver types used during the trial is also assessed using successively code only and carrier phase smoothed code measurements with the between-receiver single difference mode. Software C$^3$NAV™ (Cannon & Lachapelle, 1992) is used for this purpose. In C$^3$NAV™, parallel filters are used to control code multipath and code/carrier divergence. These filters are reset at every 300 epochs in this case. The use of a different time constant do not affect the results significantly.

Results are summarized in Table 4.10 in term of rms differences between coordinates estimated using successively code and carrier phase smoothed code, and coordinates calculated using fixed ambiguity solutions. The latter solutions are accurate to within a few cm as discussed earlier and the rms differences given in Table 4.10 represent the accuracy of the code or carrier phase smoothing solutions. The rms differences of the GPSCard™ code solutions are at the 0.5 - 1.1 m level, as compared to 2.3 - 6.0 m for the P-XII C/A code solution. The corresponding carrier phase smoothing solutions are at the 0.4 - 0.9 m level for the GPSCard™ and 0.7 - 1.0 m level for the P-XII C/A code. The GPSCard™ code and carrier phase smoothed code solutions are at the same level as the P-XII P1 or P2 solutions. These tests confirm that a sub-metre accuracy can be obtained in the marine environment using narrow correlator spacing single frequency receiver technology.

**Table 4.10: DGPS Code And Carrier Phase Smoothing Positioning Performance Statistics**

| Receiver | Observation Type | RMS Differences (m) Lat | Lon | Height |
|---|---|---|---|---|
| GPSCard™ No. 1 (Chokerings) | Code | 0.8 | 0.5 | 1.0 |
| | Code & carrier | 0.7 | 0.5 | 0.7 |
| GPSCard™ No. 2 | Code | 0.6 | 0.5 | 1.1 |
| (Chokering at Monitor only) | Code & carrier | 0.5 | 0.4 | 0.9 |
| GPSCard™ No. 3(Chokerings) | Code | 0.7 | 0.5 | 0.9 |
| | Code & carrier | 0.6 | 0.4 | 0.6 |
| P-XII C/A | Code | 3.5 | 2.3 | 6.0 |
| (Chokerings) | Code & carrier | 0.7 | 0.7 | 1.0 |
| P-XII PL1 | Code | 0.6 | 0.6 | 0.8 |
| (Chokerings) | Code & carrier | 0.3 | 0.2 | 0.4 |
| P-XII PL2 | Code | 0.5 | 0.6 | 0.8 |
| (Chokerings) | Code & carrier | 0.3 | 0.2 | 0.4 |

CHAPTER 5

# QUADRUPLE SINGLE FREQUENCY RECEIVER SYSTEM FOR AMBIGUITY RESOLUTION ON THE FLY

From Chapter 4, it is seen that resolution of carrier phase ambiguities on the fly (OTF) using a pair (monitor/remote) of single frequency receivers is difficult to achieve reliably in an operational environment due to the unfavorable ratio between carrier phase noise and multipath on the one hand, and the 19 cm wavelength of the L1 carrier on the other hand. Assuming a relatively short distance between the monitor and remote units (e.g., < 25 km, to reduce differential orbital and atmospheric effects) and the availability of at least six satellites with a PDOP ≤ 3, the time to resolution is found to vary between a few tens to 1800 seconds, depending, for one, on whether chokering groundplanes are used to minimize carrier phase multipath. In order to improve the OTF ambiguity resolution time and reliability with single frequency receivers, the use of a quadruple receiver system consisting of two static monitor units and two mobile remote units mounted on the mobile platform is investigated in this chapter. The methodology of ambiguity resolution using such a configuration is described in section 3 of Chapter 3. The ambiguities between the two monitors and between the two remote receivers can be determined within a few seconds due to the short and fixed baselines between the units. These ambiguities can in

turn be used as constraints to reduce the number of potential monitor/remote ambiguity solutions and, therefore, to reduce the time to resolution. The results of tests carried out with a configuration of four NovAtel GPSCard™ units are presented. The time to resolution of the quadruple system is compared with single pair units. The semi-kinematic results are analyzed and examined.

## 5.1 DESCRIPTION OF FIELD TEST

The semikinematic land tests were conducted on the Springbank Baseline west of Calgary using four narrow correlator spacing C/A L1 GPSCard™ units on two different occasions, namely in February and July 1993. The static initialization provided a reliable and independent reference solution for the ambiguities. This can be used to verify the on-the-fly ambiguity resolution computations. Only the kinematic portions of the trajectory were used to resolve the ambiguities OTF. The vehicle speed during the tests ranged from 50 to 100 km/h. The data was reduced with FLYKIN™.

The quadruple receiver configuration tested herein is shown in Figure 5.1, where k and □□refer to the monitor antennas and i and j to the remote antennas on the platform. The distance k - □ between the two monitor antennas was 15 and 6 m and the distance i - j between the two antennas mounted on the suburban vehicle was 1 and 2 m during test #1 and #2, respectively. During test #1, only one monitor antenna (k) was equipped with a chokering groundplane. During test #2, all four antennas were fitted with such groundplanes. The chokering groundplanes were used to reduce carrier phase mutlipath effects. The distance between the monitor stations and the vehicle did not exceed 5 km. The

differential effects of atmospheric and orbital errors are therefore cancelled out in this case.

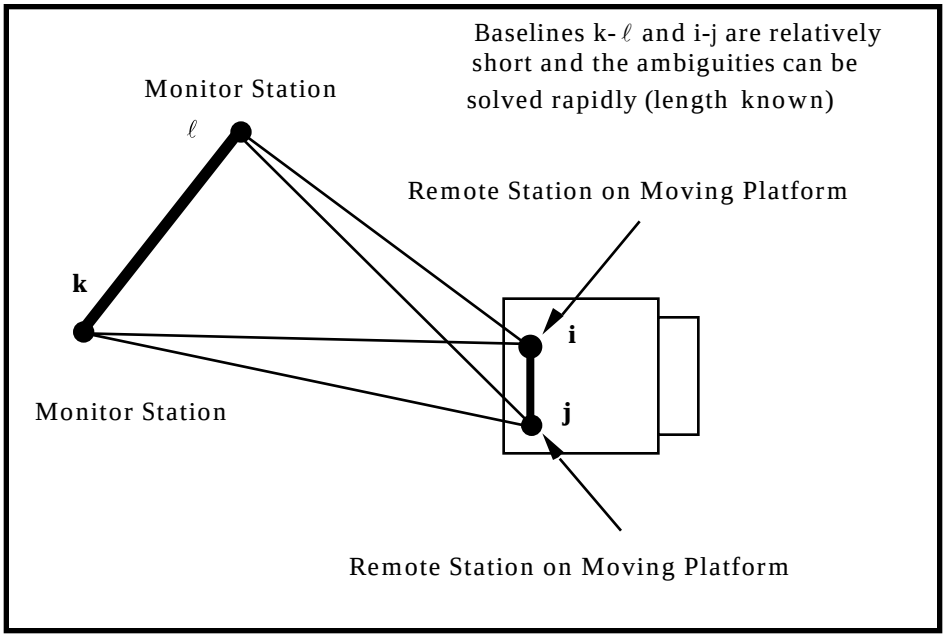


**Figure 5.1: Quadruple Receiver Configuration**

The satellite azimuths and elevations for test #1 are given in Table 5.1. Figure 5.2 shows satellite elevations for test #2. SV 19 had the highest elevation for test #1 and was used as the base satellite for all computations involving double differences. For test #2, SV 17 was selected as the base satellite. In each case, the PDOP was less than 3. The measurements were recorded every second.

**Table 5.1: Satellite Azimuths and Elevations For Test #1**

| SV | Azimuth | Elevation |
|---|---|---|
| 02 | 222 - 234˚ | 07 - 32˚ |
| 11 | 117 - 93˚ | 16 - 39˚ |
| 16 | 310 - 282˚ | 23 - 22˚ |
| 18 | 167 - 166˚ | 56 - 27˚ |
| 19 | 298 - 100˚ | 81 - 69˚ |
| 27 | 276 - 292˚ | 41 - 68˚ |
| 28 | 72 - 45˚ | 33 - 24˚ |

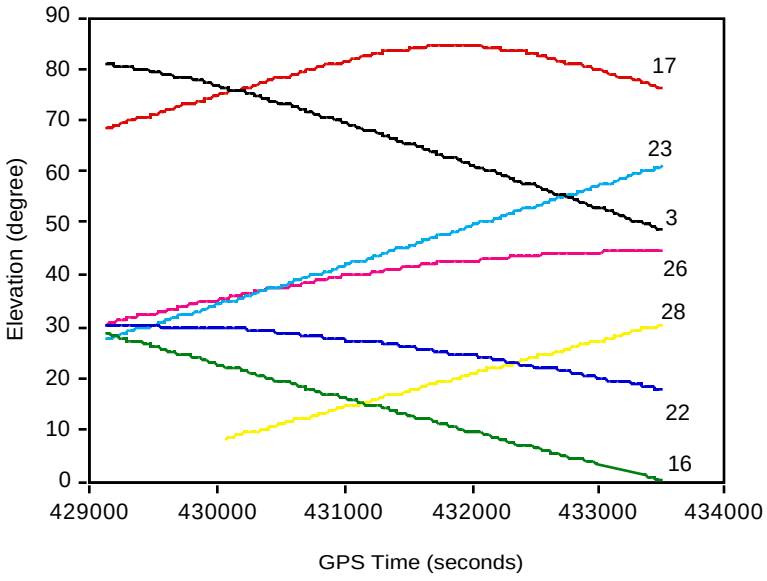


**Figure 5.2: Satellite Elevations For Test #2**

## 5.2 AMBIGUITY RESOLUTION ON THE FLY WITH SINGLE MONITOR-REMOTE PAIRS

Ambiguity resolution on the fly was first attempted using each combination of monitor-remote pairs. The double difference carrier phase observations were assigned *a priori* standard deviations of 15 and 10 mm for test #1 and #2, respectively. Some 15 to 20 trials were performed in each case by shifting the starting point forward by 60 seconds. The average observation time required was 810 and 355 seconds for test #1 and #2, respectively. The longer time required for test #1 is due to the absence of chokering groundplanes at three of the four antennas and, consequently, to higher carrier phase multipath. The success rate was 100% for all monitor/remote pairs, which indicates that the *a priori* standard deviation selected was not too optimistic.

Figures 5.3 and 5.4 show the double difference residuals for k - □, i - j, and k - i, with fixed integer ambiguity solutions for SV19-18 and SV17-03, observed during tests #1 and #2, respectively. It is evident that the residuals during test #2 are substantially lower than those obtained during test #1. For test #1, only one monitor antenna had chokering groundplanes. For test #2, all four antennas were equipped with the groundplanes. The use of chokering groundplanes is effective to mitigate multipath effects. Since the distance between the two remote units is relatively short, the carrier phase multipath between the two antennas on the vehicle is strongly correlated. This correlation can be seen in Figures 5.5 and 5.6 which show the double difference residuals of SV19-18 and SV17-03 for k - j and □ - i observed during tests #1 and #2, respectively. This correlation is expected to be much smaller if the distance between the two monitor units and that between

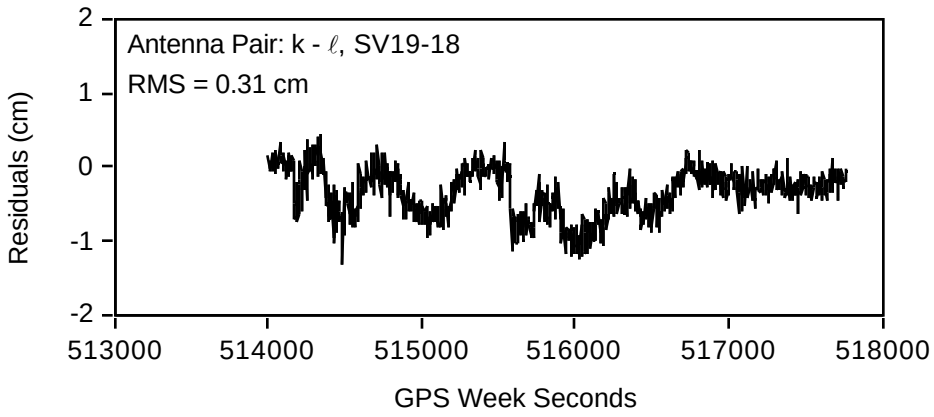


**(a) Two Monitor Antenna Pair**

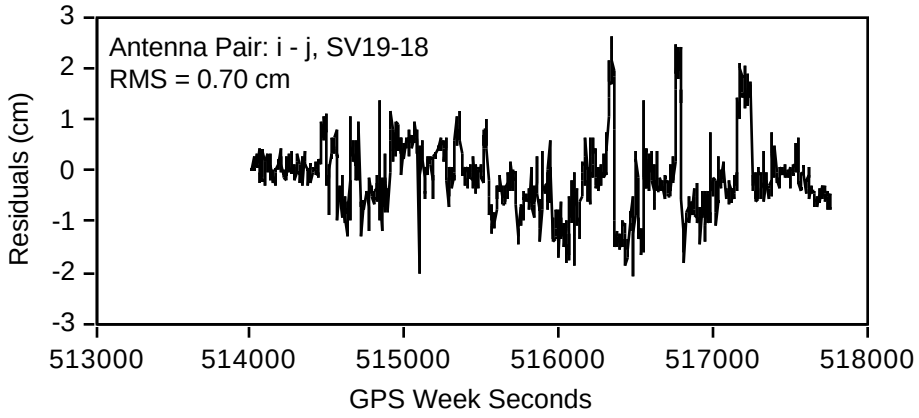


**(b) Two Remote Antenna Pair**

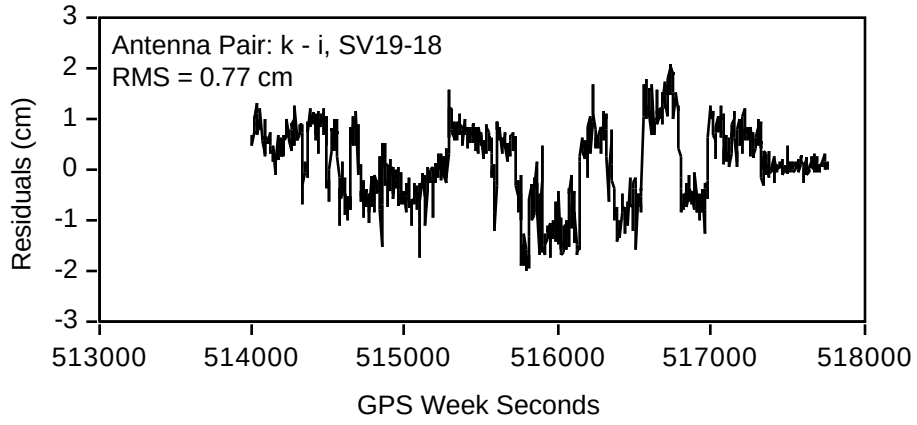


**(c) Monitor/ Remote Antenna Pair**

**Figure 5.3: $\Delta\nabla\Phi$ Residuals - Test #1 (No Chokering Groundplanes at three Antennas)**

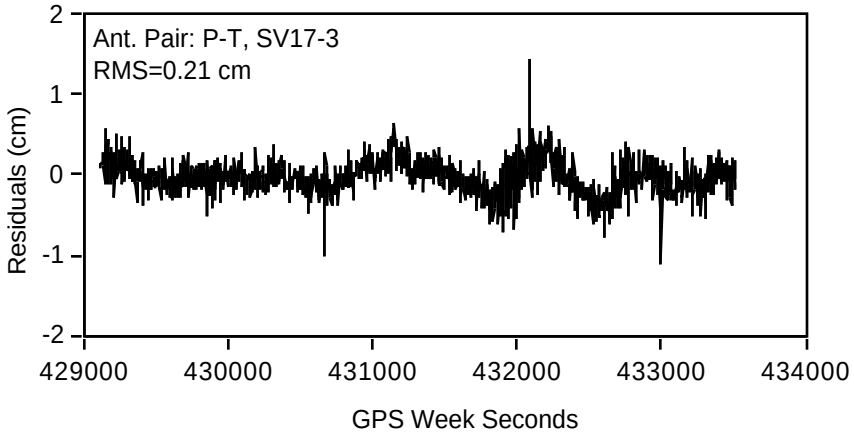


**(a) Two Monitor Antenna Pair**

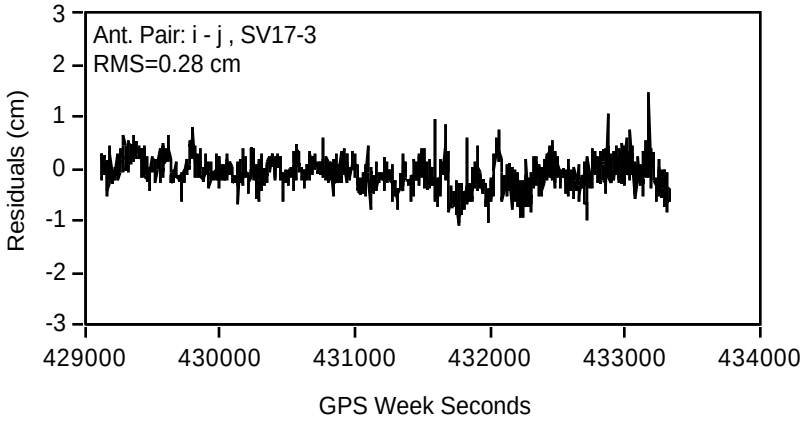


**(b) Two Remote Antenna Pair**

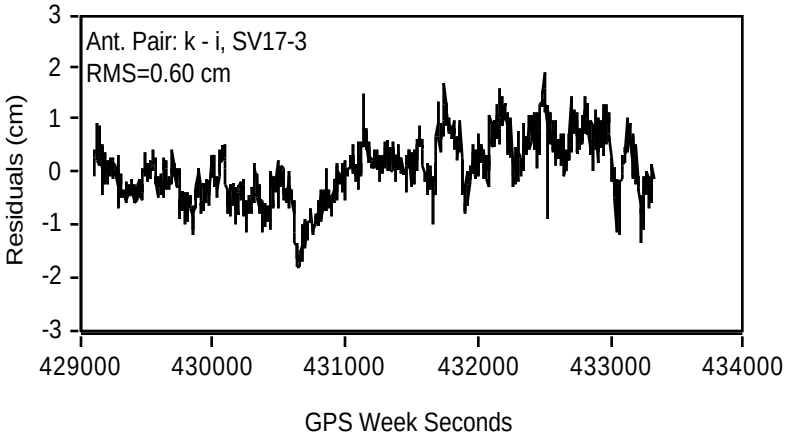


**(c) Monitor / Remote Antenna Pair**

**Figure 5.4: $\Delta\nabla\Phi$ Residuals - Test #2 (Chokering Groundplanes at all four Antennas)**

the two remote units were sufficiently long, e.g., 100 m. Although this is relatively easy to achieve on an aircraft or ship, total decorrelation cannot be achieved on a smaller platform such as a land vehicle and this will decrease the performance of the quadruple system.

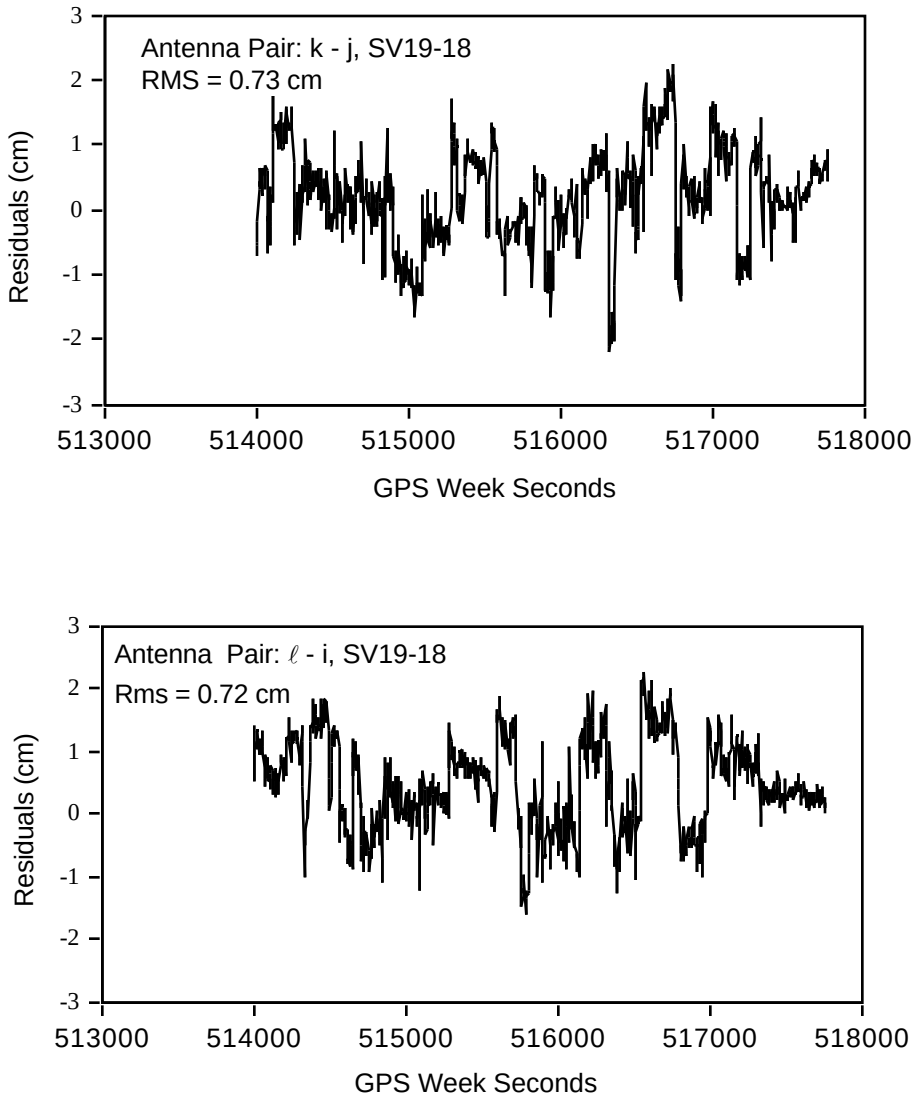


**Figure 5.5: Correlated $\Delta\nabla\Phi$ Residuals Between Pairs of Receivers, Test #1**

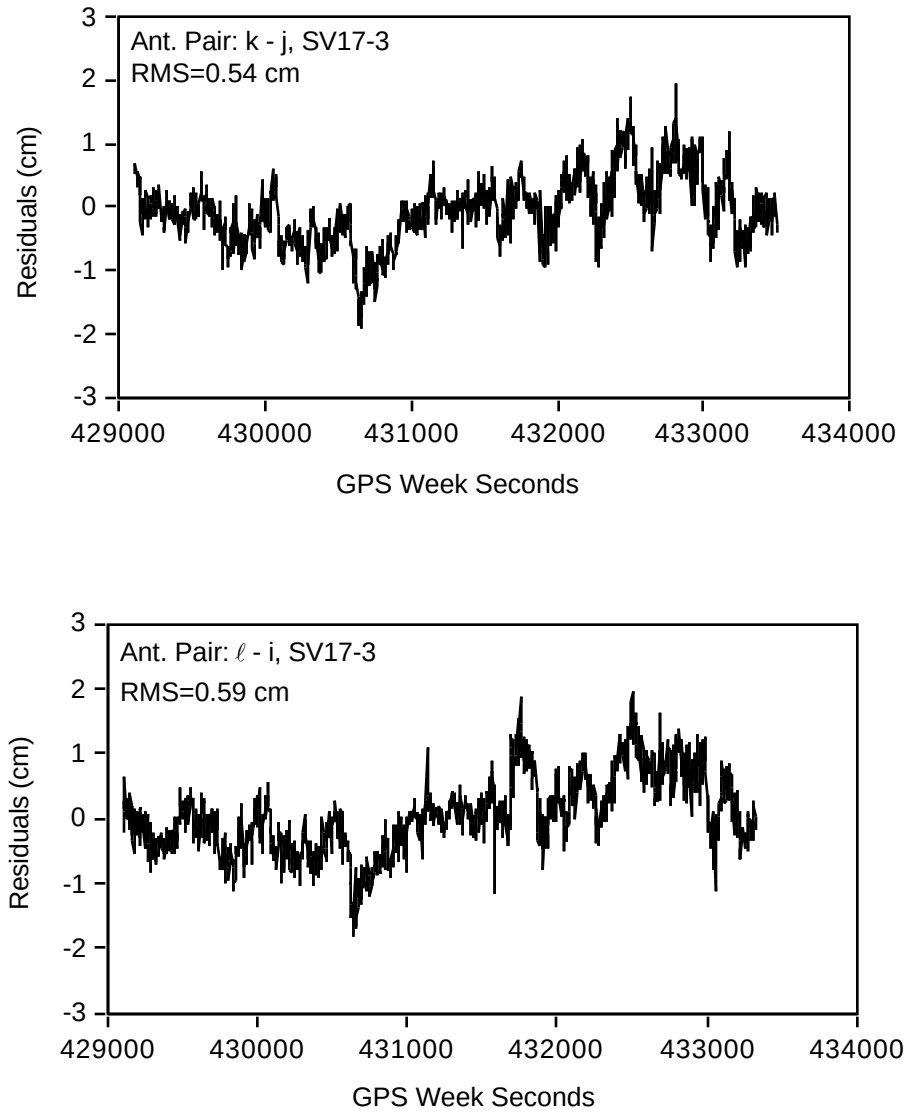


**Figure 5.6: Correlated $\Delta\nabla\Phi$ Residuals Between Pairs of Receivers, Test #2**

## 5.3 AMBIGUITY RESOLUTION ON THE FLY WITH A QUADRUPLE SYSTEM

Since the vector lengths k - □ and i - j are relatively short (< 100 m) and can be easily determined, the double difference carrier phase ambiguities $\Delta N_{k-□}$'s and $\Delta N_{i-j}$'s can be resolved reliably using a few seconds of observations. The above ambiguities can then be used as constraints in solving the double difference ambiguities between the monitor and remote receivers, e.g., $\Delta N_{i-k}$, $\Delta N_{j-k}$, $\Delta N_{i-□}$, and $\Delta N_{j-□}$. Referring to section 3 of Chapter 3, the constraints for the quadruple system shown in Figure 5.1 can be expressed as:

$$\Delta N_{i-j} = \Delta N_{i-k} - \Delta N_{j-k} \quad (5.1)$$

$$\Delta N_{i-j} = \Delta N_{i-□} - \Delta N_{j-□} \quad (5.2)$$

$$\Delta N_{k-□} = \Delta N_{k-i} - \Delta N_{□-i} \quad (5.3)$$

These three sets of double difference ambiguity relations yield (n-1)x3 double difference ambiguity equations, where n is the number of satellites observed. The potential ambiguities for each monitor-remote pair shown in Figure 5.1 are first calculated using a standard OTF procedure. Only the potential ambiguities which satisfy the above equations are retained.

The quadruple receiver configuration was analyzed using a series of 18 (test #1) and 17 (test #2) trials conducted using starting points shifted some three minutes forward from the previous one to decorrelate code and carrier receiver noise and multipath as much as possible. The summary results are given in Table 5.2. In these tests, the data from each remote-receiver pair was processed separately until the number of potential ambiguity solutions was down to 50.

Once 50 potential ambiguity solutions remained on each monitor/remote pair, the constraint equations were used to reject the solutions which did not satisfy these equations. This left 8 (test #1) and 16 (test #2) sets of potential solutions. Further processing was then done on each remote-receiver pair using these solutions until a unique solution was obtained on at least one remote-receiver pair. The constraint equations were then used to find the ambiguities of the other remote-receiver pairs. This reduced the time to resolution from 810 to 471 seconds in test #1, and from 355 to 181 seconds in test #2, a gain of 42% and 48%, respectively. The results show that a 45% improvement is obtained using the quadruple system.

**Table 5.2**

**Summary of Performance Statistics for Ambiguity Resolution On The Fly with a Quadruple GPSCard™ Configuration**

| Characteristics | Test # 1 No chokering ground-plane at 3 antennas | Test #2 Chokering ground-used at all antennas |
|---|---|---|
| Average period required for ambiguity resolution using a single pair of receivers without constraint equations | 810 | 355 |
| Average period required for each pair of receivers to go down to 50 potential ambiguity sets | 177 | 47 |
| Average number of ambiguity sets which satisfy the constraint equations (out of 50) | 8 sets | 16 sets |
| Average period required for ambiguity resolution using constraint equations | 471 | 181 |
| Average improvement of quadruple receiver configuration over single pair of receivers | 42% | 48% |

## 5.4 KINEMATIC POSITIONING RESULTS

In order to illustrate the level of accuracy achieved for the vehicle trajectory with the correct integer ambiguities held fixed, the differences between measured and known values of the control points was computed using the data collected during test #1. The vehicle trajectory from two different monitor stations was compared to give an internal performance evaluation of the different receiver combination.

As discussed earlier, the semi-kinematic (e.g., stop/go) mode was used during test #1 and three runs were done. During each run, the vehicle was brought to a stop and the antenna was moved to the control point, and one minute of observations were made. The double difference phase ambiguities were selected the results of ambiguity resolution for quadruple system. The vehicle trajectory was estimated by a Kalman filter with fixed ambiguities. Tables 5.3 and 5.4 show the agreement at the control points during each run for receiver pairs k-j and □ - i, respectively.

Differences with known control points vary between -4 and 2 cm and are consistent with the accuracy of the control points. The mean values computed using the differences with the known control points are 0.2 cm in latitude, -0.8 cm in longitude and -1.4 cm in height. The results are satisfactory and indicate that the kinematic position with carrier phase are accurate to the cm level.

The differences of vehicle trajectory from two different monitor stations is shown in Figure 5.7. It is seen that the differences in latitude and longitude are generally within 1.0 cm, but in height go up to 2.0-3.0 cm. The rms are 0.3 cm in

latitude, 0.2 cm in longitude and 1.0 cm in height, respectively. The results provide a good check of the processing method and receiver performance.

**Table 5.3: Position Differences with Control Points for Receiver Pair: k - j**

| Control Points - Kinematic Coordinates<br>Receiver Pair : k - j | | | | | | | | | |
|---|---|---|---|---|---|---|---|---|---|
| Run | Δφ | | | Δλ | | | Δh | | |
| | Max. (cm) | Min. (cm) | Mean (cm) | Max. (cm) | Min. (cm) | Mean (cm) | Max. (cm) | Min. (cm) | Mean (cm) |
| No. 1 | 0.02 | -0.92 | -0.49 | -0.62 | -1.07 | -0.62 | 0.40 | -1.16 | -0.44 |
| No. 2 | 0.03 | -0.59 | -0.28 | -0.68 | -1.28 | -0.99 | -1.02 | -2.97 | -1.98 |
| No. 3 | 0.95 | 0.22 | 0.57 | -0.67 | -1.14 | -0.89 | -0.50 | -2.10 | -1.24 |

**Table 5.4: Position Differences with Control Points for Receiver Pair: □□-i**

| Control Points - Kinematic Coordinates<br>Receiver Pair: ℓ - i | | | | | | | | | |
|---|---|---|---|---|---|---|---|---|---|
| Run | Δφ | | | Δλ | | | Δh | | |
| | Max. (cm) | Min. (cm) | Mean (cm) | Max. (cm) | Min. (cm) | Mean (cm) | Max. (cm) | Min. (cm) | Mean (cm) |
| No. 1 | 0.85 | -0.37 | 0.25 | -0.52 | -1.20 | -0.87 | -0.49 | -3.41 | -2.23 |
| No. 2 | 1.22 | 0.55 | 0.86 | -0.63 | -1.21 | -0.87 | -1.77 | -3.38 | -2.58 |
| No. 3 | 0.78 | -0.10 | 0.31 | -0.56 | -1.10 | -0.80 | -1.77 | -3.20 | -2.45 |

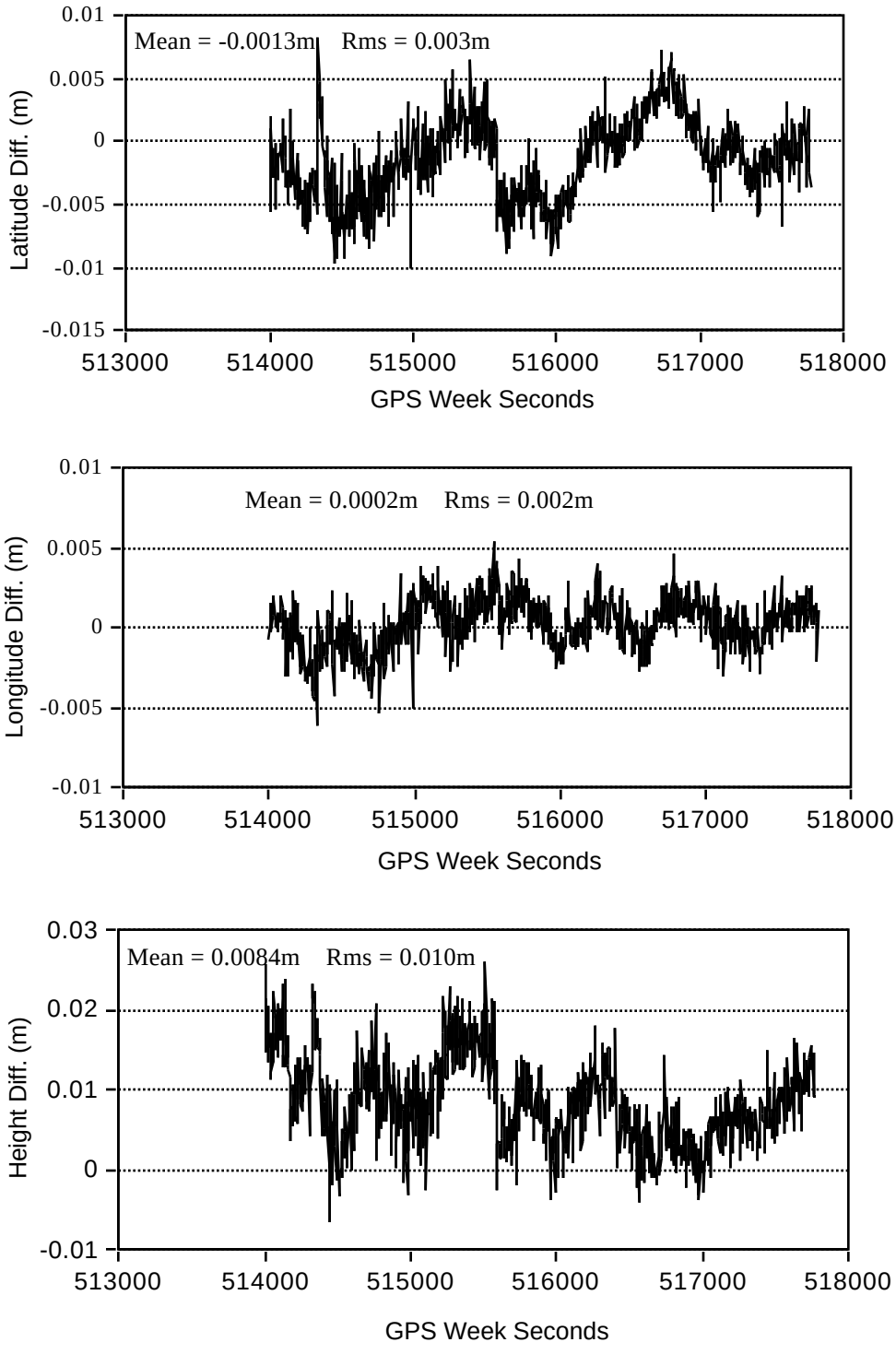


**Figure 5.7: The Vehicle Trajectory Differences form Two Different Monitor Stations**

CHAPTER 6

# APPLICATION OF GPS TO PRECISE WATER LEVEL PROFILING

The application of GPS to water level profiling with cm-level accuracy is investigated in this chapter with the ambiguities resolved on the fly. In order to study the possibility, a DGPS survey along an 80-km section of the Fraser River, British Columbia, was carried out in March 1993. Dual frequency receivers were used to permit quasi-instantaneous carrier phase ambiguity resolution OTF using widelane observables. Frequent ties to Bench Marks (B.M.'s) were made to assess independently the accuracy of the GPS methodology. The shore-to-launch height transfer through spirit leveling was used. From the results presented in this chapter, it is demonstrated that the precise DGPS positioning can be used as a tool for profiling river water levels at the 5-10 cm accuracy level. The knowledge of continuous water level profiles can be applied to tidal studies and other hydrographic purposes such as the establishment of chart datums.

Field work conducted and data pre-processing are first described. The DGPS positioning results for the static reference stations are then presented. The kinematic water level profiling results and the accuracies obtained are discussed. The performance of the solutions for long distances between the GPS reference station and the survey launch is also investigated. The results of this project are described by Lachapelle et al (1993d).

## 6.1 FIELD MEASUREMENTS AND DATA PREPROCESSING

The GPS survey of an 80-km segment of the Fraser River, British Columbia, from its mouth in the Strait of Georgia to Chilliwack, as shown in Figure 6.1, was conducted during the period 15 - 18 March 1993. A 13-m survey launch (Revisor) moving at a speed of about 10 km $h^{-1}$ was used. The P code was transmitting in the clear and Ashtech P-XII receivers were used to collect code and carrier phase data on both L1 and L2 simultaneously. Widelane observables (L1 - L2) could therefore be used to resolve the carrier phase ambiguities on-the-fly effectively. One receiver was mounted on the launch and three others were deployed at five reference stations, as shown in Figure 6.1. The three-dimensional coordinates of these reference stations were estimated through a precise GPS static survey.

Accurate levelled or orthometric heights were transferred effectively to shore B.M.'s for direct access by survey launch-borne GPS. The locations of the B.M.'s are shown in Figure 6.1. These B.M.'s were subsequently used to assess independently the accuracy of GPS-derived orthometric heights. The GPS-derived ellipsoid height differences were converted to orthometric height differences using a geoid model.

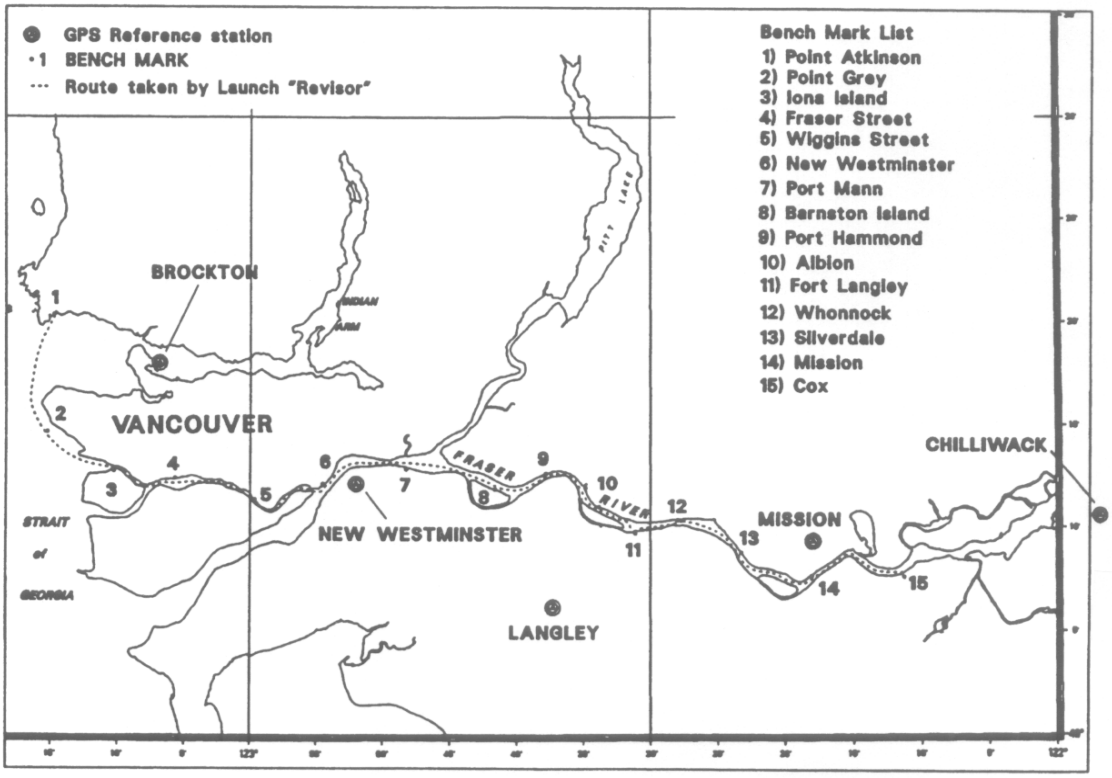


**Figure 6.1: Fraser River GPS Water Level Profiling Survey**

Two chokering groundplanes were available during the river survey. These were previously found to improve significantly the performance of the P-XII receiver (Cannon & Lachapelle, 1992a). One was used with the receiver on the survey launch every day, except on 17 March. The other was used at reference station Langley on 15, 16 and 17 March, and at station Mission on 18 March. The maximum distance between the launch and any one reference station used initially was < 20 km. During the survey, 4 to 7 satellites at an elevation ≥ 15˚ were available. The data was utilized only when the number of satellites was ≥ 5 since ambiguity resolution on the fly requires at least 5 satellites. The PDOP was generally between 2 and 5, except for short periods during which it was larger due to losses of carrier phase lock. The observed numbers of satellites and

PDOP for 15, 16, 17 and 18 March are shown in Figures 6.2 to 6.5, respectively. Several bridges and other interference sources, especially in the vicinity of Vancouver International Airport, resulted in losses of phase lock. The ambiguities could however be recovered quickly using the widelane observables.

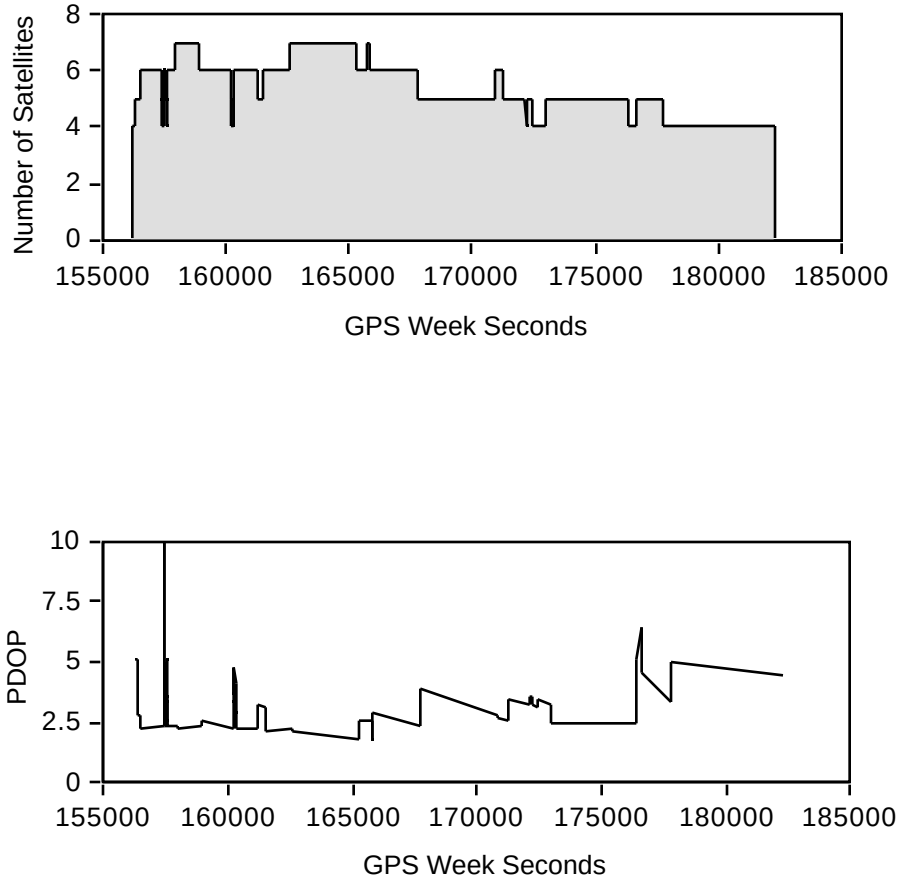


**Figure 6.2: Observed Numbers of Satellites and PDOP, 15 March 1993**

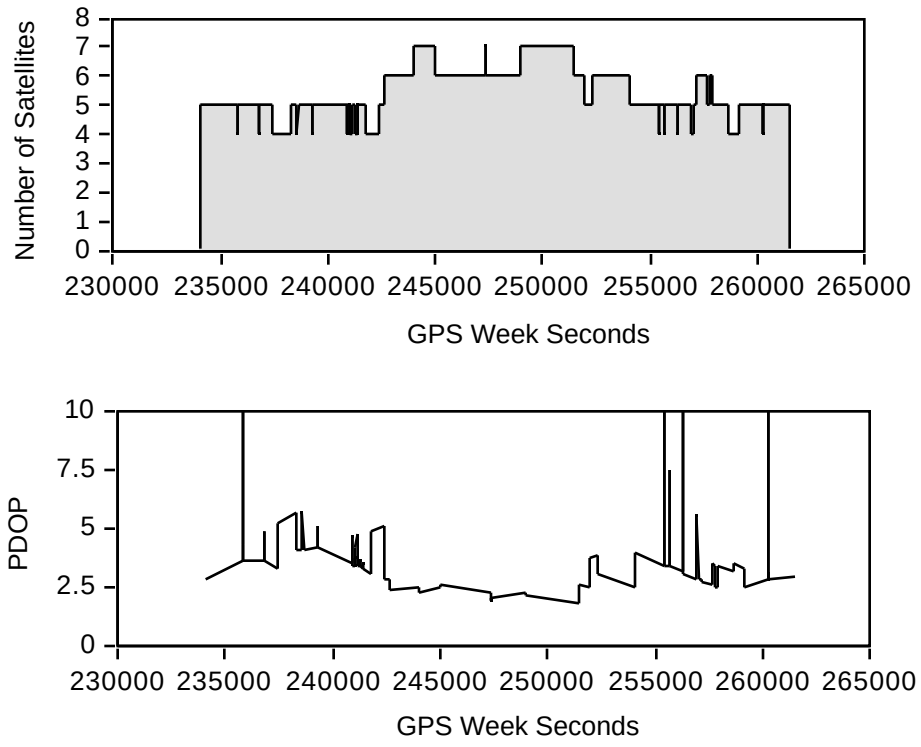


**Figure 6.3: Observed Numbers of Satellites and PDOP, 16 March 1993**

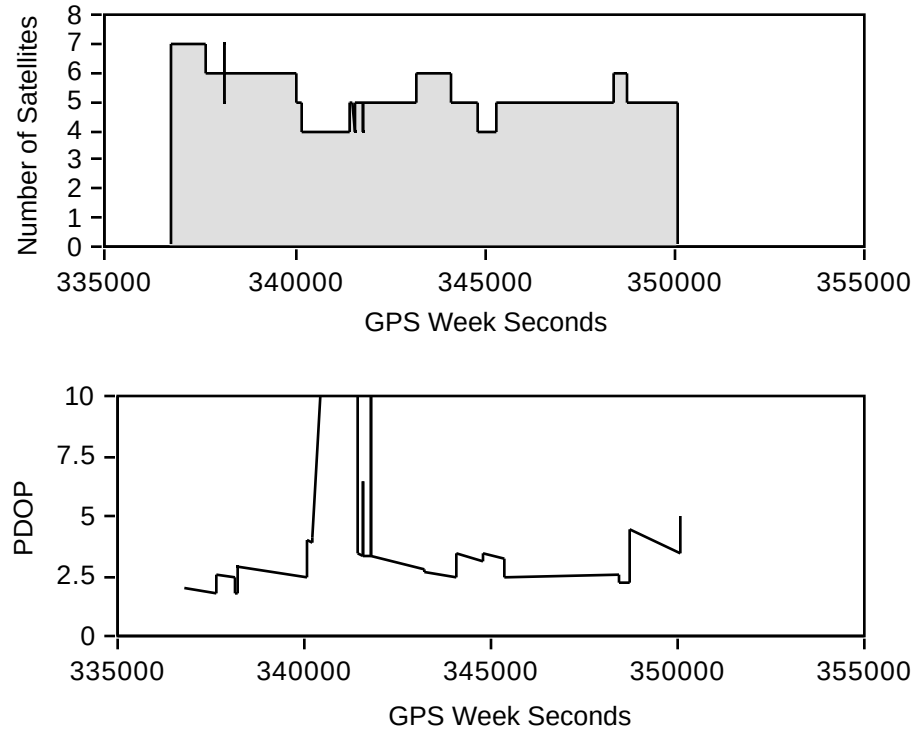


**Figure 6.4: Observed Numbers of Satellites and PDOP, 17 March 1993**

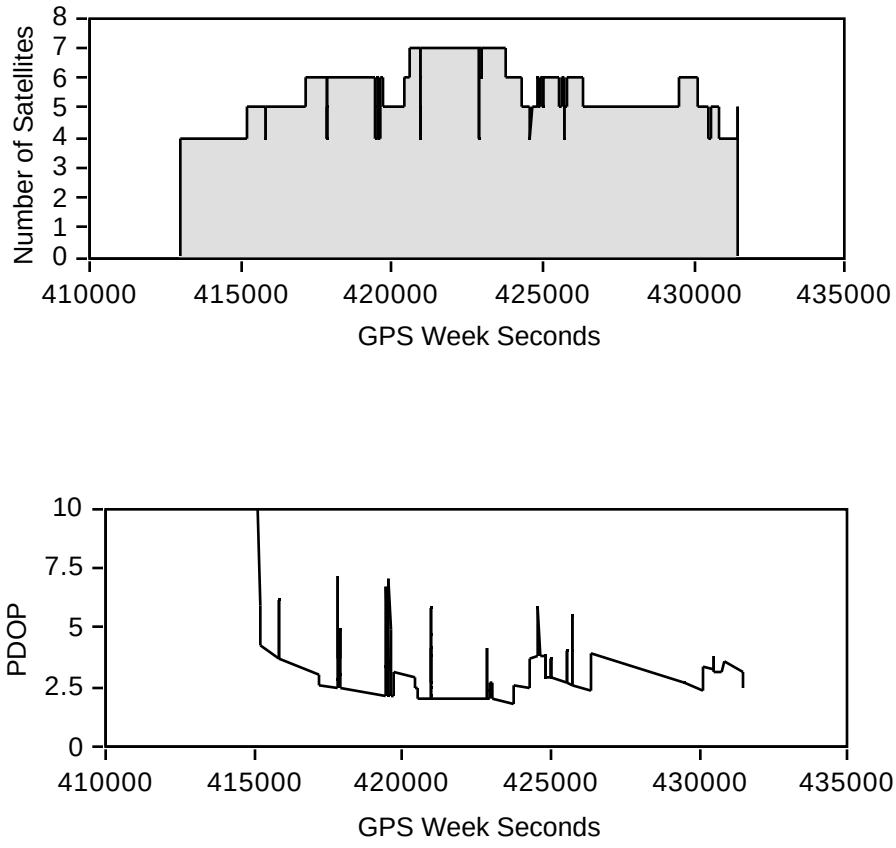


**Figure 6.5: Observed Numbers of Satellites and PDOP, 18 March 1993**

Data preprocessing was made for cycle slip detection. It was found that the data collected on 15 and 18 March proved to be of a better quality than that on 16 and 17 March. In the former case, segments of up to 10 minutes of cycle slip free data were recorded. In the latter case, cycle slips, mostly on L2, were detected every 10 to 30 seconds. These problems are likely caused by a combination of factors, such as the absence of a chokering groundplane on the launch on 17 March, frequently passing through bridges on 16 March and receiver instabilities. These problems were overcome by using the widelane

observables (L1-L2) since widelane carrier phase ambiguities can be resolved effectively, is seconds.

## 6.2 POSITIONING RESULTS FOR REFERENCE STATIONS

The static data processing was firstly carried out prior to implementing the kinematic data. The double difference solution was retained as the best solution. A total of 6 points were observed. Two of them, Brocton and Mission Geodetic Point, were selected as fixed site since their coordinates (WGS 84) were obtained from the Canadian Hydrographic Service (CHS). All other coordinates refer to these two stations. Table 6.1 gives the stations observed and processed in static mode. The sketch of the reference stations is shown in Figure 6.6.

**Table 6.1: Stations observed in Static Mode**

| Station | March 15 | March 16 | March 17 | March 18 |
|---|---|---|---|---|
| Brockton | | ** | | ** |
| Mission Geodetic Point | | | ** | |
| New Westminster | ** | ** | | * |
| Langley | ** | ** | ** | |
| Mission | ** | | ** | ** |
| Chilliwack | | | ** | |

Note: ** station observed and processed.
* station observed but not processed.

Table 6.2 lists the coordinates of the reference stations as determined from the DGPS survey. At least 6 hours of data were recorded at all reference stations except for the Mission Geodetic Point. Only some one hour of observation was conducted at the Mission Geodetic Point. However, it is enough to determine the baseline between the Mission Geodetic Point and Mission reference station since the distance between these two points is only some 3 km. The lengths of other baselines are more than 20 km. The solutions with fixed integer ambiguities for short baselines and float ambiguities for long baselines were used as the final results. The carrier phase data interval used in the static data reduction was 4 seconds for the short baselines and 15 seconds for the long baselines. The satellite elevation cutoff angle was 15°.

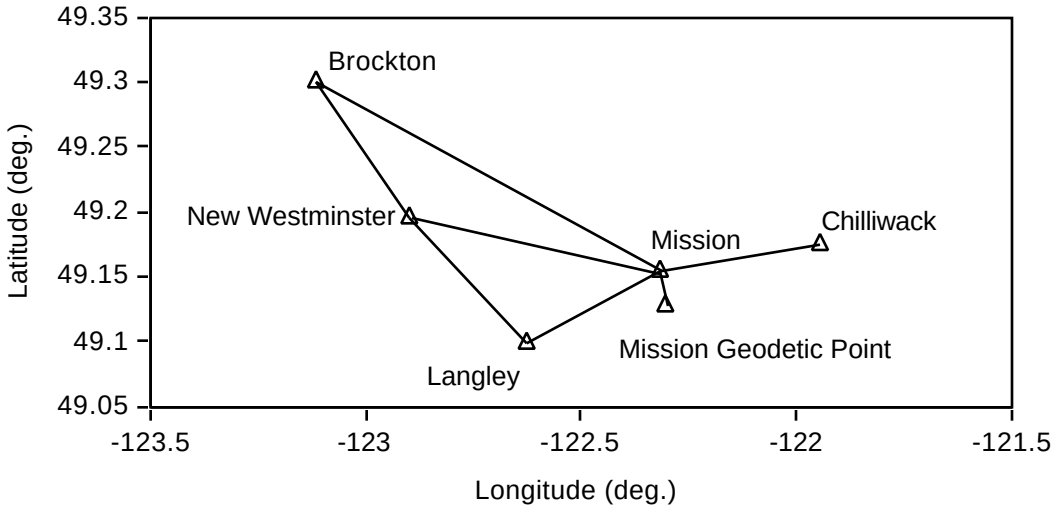


**Figure 6.6: Sketch of the Reference Stations**

**Table 6.2: DGPS Static Survey Results for Reference Stations**

| Stations | Day | Baselines | Latitude (N) (dms) | Longitude(W) (dms) | Ellipsoidal Height (m) |
|---|---|---|---|---|---|
| Mission | March 15 | MiGeoP[1]-Mission | 49-09-20.87842 | 122-18-53.51087 | 128.972 |
| | March 18 | Brocton-Mission | 49-09-20.86790 | 122-18-53.50542 | 128.956 |
| New Westminster | March 15 | Mission-New Wm[2] | 49-11-48.34504 | 122-53-58.98030 | -17.434 |
| | March 16 | Brocton-New Wm[2] | 49-11-48.34453 | 122-53-58.98379 | -17.401 |
| Longley | March 15 | Mission-Langley | 49-06-02.83482 | 122-37-34.63107 | -8.394 |
| | March 16 | Brocton-Langley | 49-06-02.83377 | 122-37-34.62637 | -8.391 |
| | March 17 | Mission-Langley | 49-06-02.83285 | 122-37-34.63167 | -8.340 |
| Chilliwack | March 17 | Mission-Chilliwack | 49-10-37.56116 | 121-56-35.58154 | -6.853 |

Note: 1 MiGeoP represents Mission Geodetic Point
2 New.Wm represents New Westminster reference station

The misclosures of two triangles formed by the baseline solutions were examined. The results are presented in Table 6.3. From this table, it is seen that the misclosure in each component is less than 15 cm. The 3D error is at the 1.0 ppm level, which is well within expected accuracy.

**Table 6.3: Triangle Misclosures of Baseline Solutions**

| Triangle | Misclosure ($\phi$) | Misclosure ($\lambda$) | Misclosure (h) | Length (km) | 3D Error m / ppm |
|---|---|---|---|---|---|
| Brockton-Mission-New Westminster | 0.015 m | -0.108 m | -0.033 m | 122 km | 0.114 / 0.9 |
| Brockton-Mission-Langley | 0.032 m | 0.145 m | -0.004 m | 125 km | 0.148 / 1.1 |

It should be mentioned that the DGPS derived ellipsoidal differences must be converted to orthometric height differences prior to comparison with levelling heights. The relation between these two height systems can be given by

$$N = h - H \tag{6.1}$$

Where h ... ellipsoidal height

H ... orthometric height

N ... geoidal height

In this case, two kinds of geoid models are available. One was provided by Geodetic Survey of Canada (Veronneau & Mainville, 1992) and another geoid model was computed at The University of Calgary (She, 1993). A comparison with these two models at a few points resulted in a relative agreement of better than 2 cm. This however does not mean that the geoid is known to such a high level of accuracy since essentially the same gravimetric data was used for both models. The agreement between levelled and GPS-derived orthometric heights will however provide a measure of the accuracy of the relative geoid along the Fraser River.

## 6.3 KINEMATICS RESULTS FOR WATER LEVEL PROFILING

The GPS kinematic data was post-processed using carrier phase ambiguity resolution on the fly and software FLYKIN™. The nearest reference station was usually used to form the double differenced carrier phase observables. The double differenced widelane observables were assigned *a priori* values of 3 cm on 15, 16, and 18 March, and 3.5 cm on 17 March since chokering groundplanes were not used on the survey launch on that day. The time to integer ambiguity

resolution on-the-fly varied between a few seconds to a few minutes, depending upon the satellite geometry and on the carrier phase noise and multipath. As discussed early, cycle slips occurrences were frequent due to the dynamics of the survey launch and receiver instabilities. These problems were overcome by constraining the GPS-derived height differences along the trajectory to ≤ 50 cm over short periods. When using widelane observables, the wavelength is 86 cm and the above constraint is effective in detecting a cycle slip and speeding up ambiguity resolution on the fly. Sample double differenced widelane carrier phase residuals for each day of the survey are shown in Figure 6.7. The RMS values range from 0.9 cm for 15 March to about 2.0 cm for the other days. The reason for better residuals on 15 March is the use of chokering groundplanes at both the remote unit on the survey launch and at the reference station to reduce phase multipath.

Table 6.4 lists the differences between levelled and GPS derived heights at B.M.'s along Fraser river. Table 6.5 summarizes the statistics of the results. In this case, four kinds of agreements are examined. The first one is the agreement between successive GPS height determinations at each B.M. visit. The second one is the agreement between successive B.M. visits. Then, the agreement between GPS-derived and levelled heights at each B.M. is examined. Finally, the agreement between GPS-derived and levelled heights at each B.M. is estimated again after a geoid bias is removed.

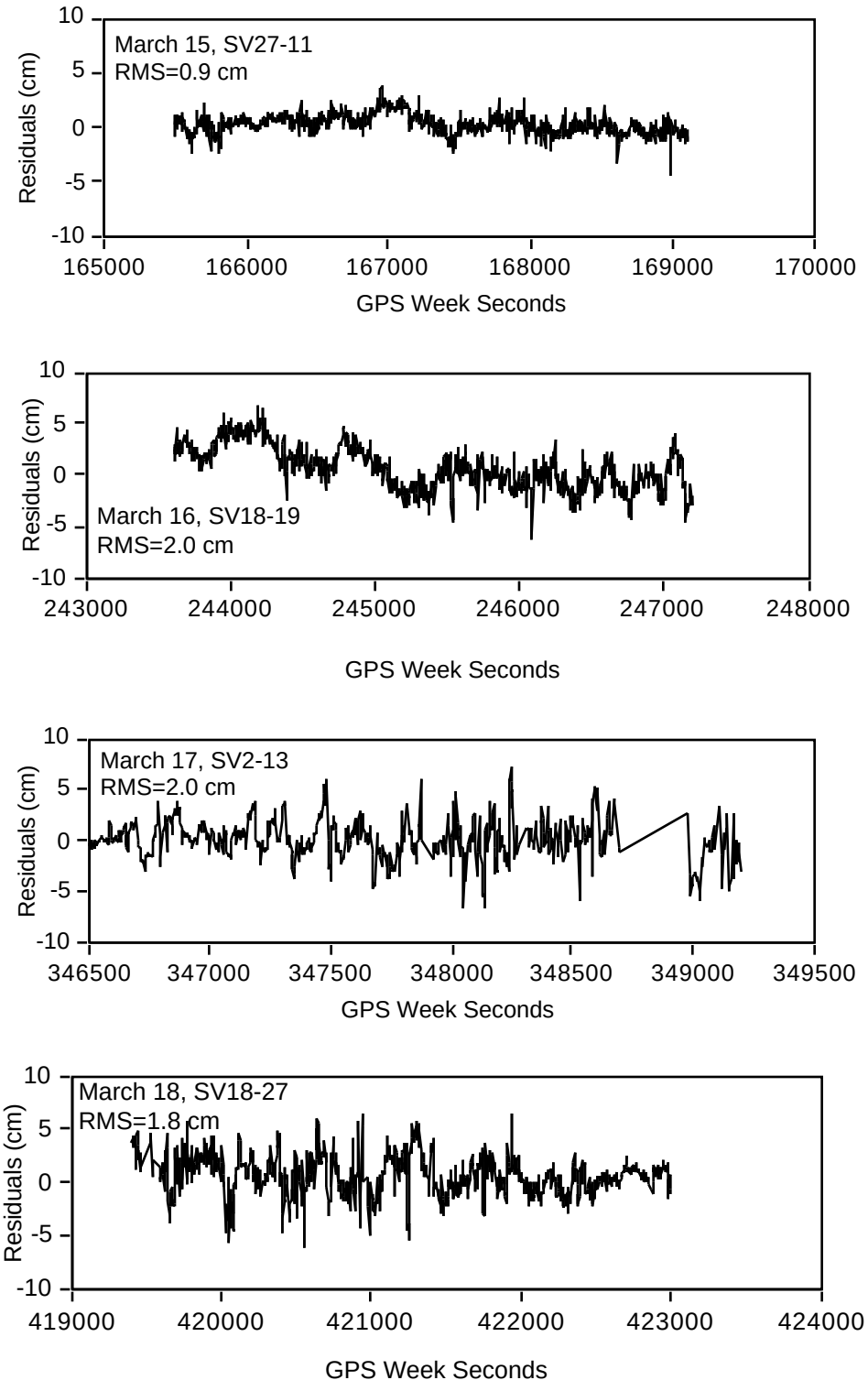


**Figure 6.7: Double Difference Carrier Phase Residuals With Integer Ambiguities Resolved On the Fly**

The procedure used to transfer GPS-derived heights to the B.M.'s on shore was carried out using a level on shore and a levelling rod on the launch. Readings of the rod from the shore, with the launch either moving or at rest, were made several times at every B.M., at intervals of ≤ 200 s. The observation time was recorded to determine the GPS antenna height at that epoch during post-processing. The height offset between the GPS antenna and the rod was also determined. The distance between the level and the rod was usually < 50 m. This height transfer, which is the largest error of all those contributing to the estimation of the GPS antenna elevation by land-based spirit levelling, was estimated independently at 2 cm. The other errors, such as spirit levelling errors, are negligible as compared to the above. The height differences between GPS and levelling, obtained during successive rod readings, can be analyzed to determine the combined effect of the height transfer error and the GPS height stability over time at each B.M. (200 to 600 seconds) required for the height transfer. It is found that the RMS agreement between the readings is 5.2 cm.

Let us determine independently the GPS error contributions. The RMS values of the double differenced widelane phase residuals, which represent the combined effect of phase noise and multipath, is of the order of 1 to 2 cm. The PDOP varies between 2 and 5, with an average value near 3. The *a priori* GPS height stability is therefore of the order of 4.5 cm. Once the height transfer error of 2 cm is quadratically added to the above, one obtains a total error of about 5 cm, which agrees well with the empirically derived above value of 5.2 cm.

Of the 14 B.M.'s for which GPS solutions were obtained, 9 were re-visited, either later on the same day or on a different day, as indicated in Table 6.4. Some B.M.'s were visited for which no GPS solution was obtained due to an insufficient (< 5) number of satellites available. The repeatability of these measurements was assessed and the agreement between GPS-derived heights obtained at the same B.M.'s on different visits was estimated. This quantity is free from any geoid error and is an effective measure of the repeatability of GPS. The RMS agreement was found to be 5.5 cm, nearly the same as the agreement between successive determinations within a visit.

The RMS agreement between GPS-derived and levelled orthometric heights was found to be 6.4 cm. This includes possible unmodelled geoid effects. As a first approximation of such an effect, the mean difference between the two sets of heights was calculated. The value was found to be 0.6 cm. The GPS-derived orthometric heights were corrected for this geoid bias and are shown in Figure 6.8. The new RMS value is still 6.4 cm. It is well within the accuracy levels anticipated.

Sample water level profiles for March 15 and 18 are shown in Figure 6.9 and 6.10, respectively. They are the ellipsoidal heights of the GPS antenna on the survey launch when the survey launch traveled along the Fraser River. It clearly indicates that water level profiles are precisely determined. It is noted that the plots in these figures are decimated by a factor of five to reduce the density of the lines.

## Table 6.4: Differences Between Levelled and GPS-Derived Heights at B.M.'s Along Fraser River

| Bench Mark | Differences (δ) Between Levelled and GPS-Derived Orthometric Heights (cm) | | | | | | | |
|---|---|---|---|---|---|---|---|---|
| | 15 March | | 16 March | | 17 March[c] | | 18 March | |
| | (km)[a] | δ (cm)[b] | (km) | δ (cm) | (km) | δ (cm) | (km) | δ (cm) |
| Pt. Atkinson | | | 11[1] | -5, -6, -3 | | | | |
| Iona | | | | | | | 11[1] | -6, -14 |
| Fraser St | | | 14[2] | 3, 4, -1 | | | 11[1] | 7 |
| Wiggins St. | | | 5[2] | 7, 0, 5 | | | 5[2] | 3, 1, 5 |
| New West | 23[3] | 1, -2, -4 | | | | | 1[2] | 2, 3, -4 |
| Port Mann | 20[3] | 5, 6, 4 | | | | | 6[2] | 2, -3, -5 |
| Barnston Island | 12[3] | -5, -5, -2 | | | | | | |
| Port Hammond | 11[3] | 2, -2, 1 | | | | | | |
| Albion | 10[3] | -3, 2, 0, 5 | | | | | | |
| | 10[3] | -1, -7 | | | | | | |
| Fort Langley | 10[3] | 4, 5, -2 | | | | | | |
| | 10[3] | -4, -7, -3 | | | | | | |
| Whonnock | 13[3] | -5, -3 | | | 13[3] | 14, -5, -7 | | |
| Silverdale | | | | | 18[3] | 4, 12, 13 | | |
| | | | | | 18[3] | -2, 5, -2 | | |
| Mission | | | | | 4[4] | -14, -17, -16 | | |
| | | | | | 4[4] | -11 | | |
| Cox | | | | | 9[4] | 4, 0, 9 | | |

a Distance to nearest GPS reference station used
b Differences for successive measurements made up to 200 seconds apart
c No chokering groundplane on the survey launch
1 Distance from GPS Reference station Brockton (No chokering groundplane used)
2 Distance from GPS Reference station New Westminster (No chokering groundplane used)
3 Distance from GPS Reference station Langley (Chokering groundplane used on 15, 16, and 17 March)
4 Distance from GPS Reference station Mission (Chokering groundplane used on 18 March)

**Table 6.5: Statistics of GPS-Derived and Levelled Heights - Summary Statistics**

| | |
|---|---|
| RMS agreement between successive GPS height determinations ($\Delta T \leq 200$ s) at each B.M. visit. | 5.2 cm |
| RMS agreement between successive B.M. visits (several hours < $\Delta T$ < 3 days). | 5.5 cm |
| RMS agreement between GPS-derived and levelled (B.M.) heights. | 6.4 cm |
| Geoid undulation bias ($\Delta N$) estimated by comparing GPS and levelled heights. | 0.6 cm |
| RMS agreement between GPS-derived and levelled (B.M.) heights (Geoid bias removed) | 6.4 cm |

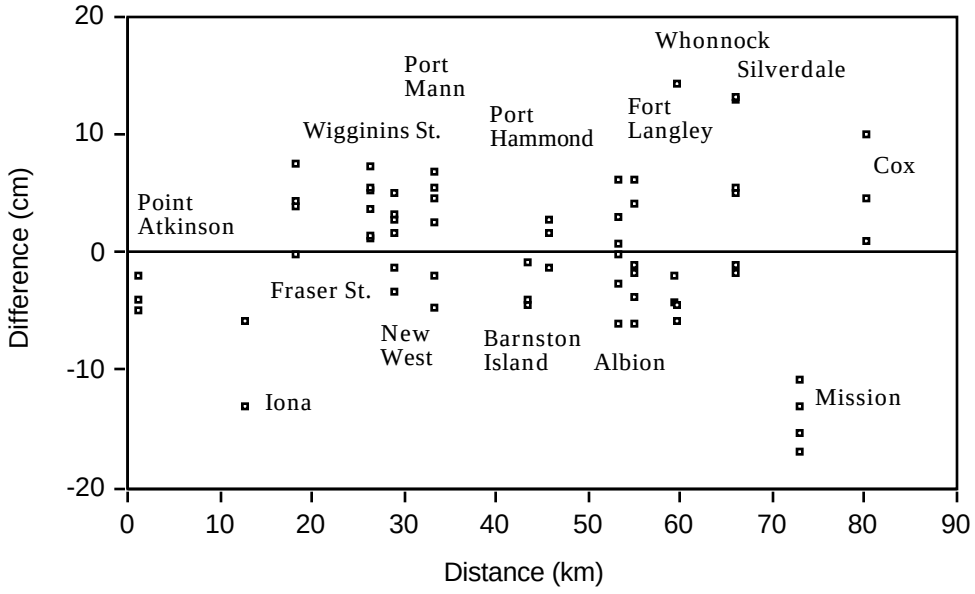


**Figure 6.8: Differences Between GPS-Derived and Levelled Heights (Geoid Bias Removed)**

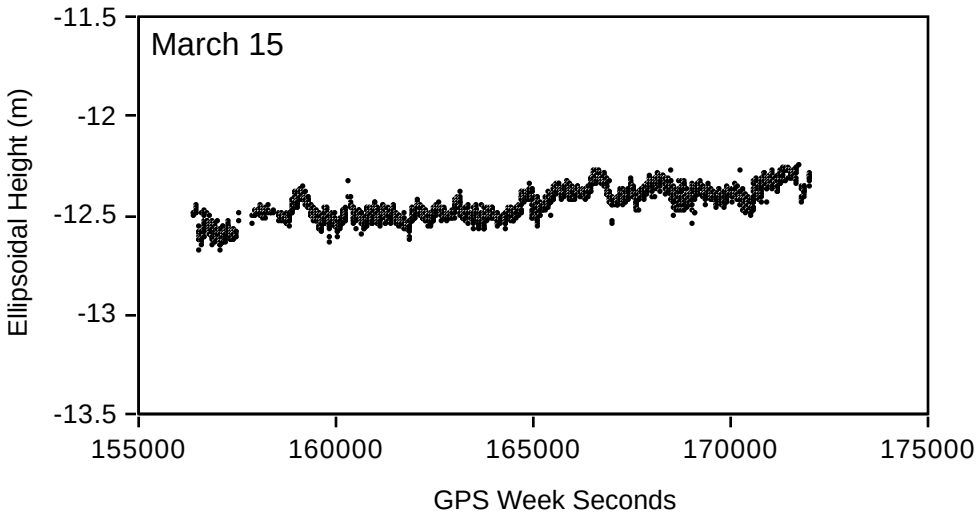


**Figure 6.9: Water Level Profiling for March 15**

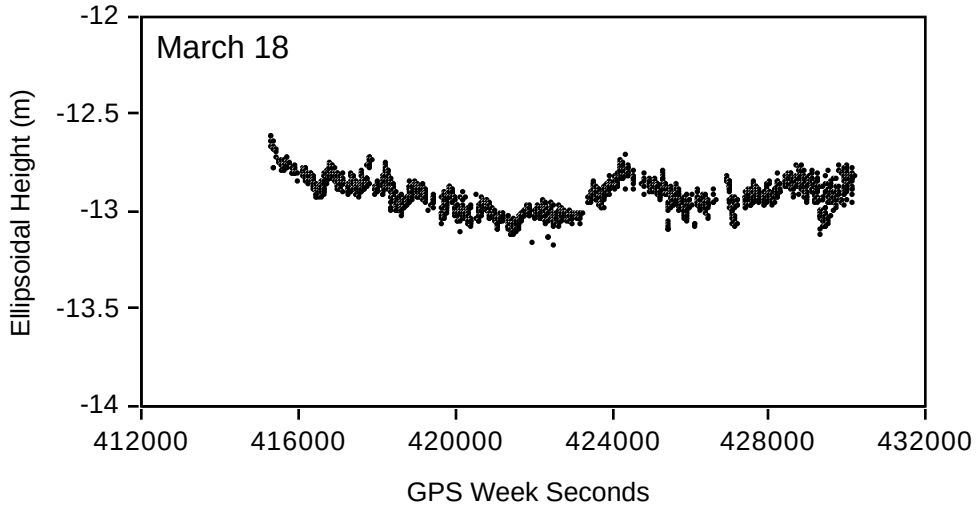


**Figure 6.10: Water Level Profiling for March 18**

## 6.4 PERFORMANCE OF WATER LEVEL PROFILING FOR LONG DISTANCE SOLUTIONS BETWEEN GPS REFERENCE STATION AND SURVEY LAUNCH

The results of water level profiling for the previous section are for the cases when the distance between GPS reference station and survey launch is ≤ 25 km. An interesting question is the performance of water level profiling when the distance between the reference station and the survey launch is greater than 25 km and up to 70 km. The GPS data on March 18 is selected to investigate this question.

The comparison of height differences between short and long distances is presented in Table 6.6. For the case of long distance solutions, the Mission reference station was used and produced distances of 38 to 65 km to the five B.M.'s listed in the table. The degradation of accuracy is gradual, with a RMS of 15.3 cm for differences between GPS-derived and levelled (B.M.) heights when using long distances versus 5.6 cm when using short distances. This is expected in view of the residual effects of the atmosphere and orbits. The results , however, are useful to understand the performance of long monitor-launch distance for ambiguity resolution on the fly.

The survey launch coordinates differences between short and long distances are given in Figure 6.11. The corresponding rms are 9.3 cm in latitude , 9.4 cm in longitude and 16.6 cm in height. The data gaps in this figure are due to the survey launch passing under bridges or ambiguities which cannot be resolved owing to the effects of atmosphere, orbits and multipath and the quality of the GPS observed data, as discussed earlier. The sudden jumps are more than

likely due to incorrect ambiguities. However, these results indicate the level of accuracy achievable when distances of up to 70 km between the GPS reference station and the survey launch for ambiguity resolution on the fly.

**Table 6.6: Comparison of Longer and Shorter Distance Solutions Between Reference Station and Survey Launch for the Height Differences**

| Bench Mark. | Distance (Km) | Time of Short (GPS Seconds) | Ellipsoidal Hgt. Diff.[1] | Diff. (GPS Derived minus Levelled) Long | Short[2] |
|---|---|---|---|---|---|
| | | 418173.0 | 19 cm | -17 cm | 2 cm |
| Port Mann | 38.2 | 418246.0 | 13 | -16 | -3 |
| | | 418366.0 | 23 | -28 | -5 |
| | | 419794.0 | 26 | -24 | 2 |
| New West | 43.6 | 419881.0 | 20 | -17 | 3 |
| | | 420211.0 | -4 | 0 | -4 |
| | | 422314.0 | 4 | -1 | 3 |
| Wiggins St. | 47.8 | 422375.0 | 3 | -2 | 1 |
| | | 422467.0 | -13 | 18 | 5 |
| Fraser St. | 56.8 | 424850.0 | 20 | -13 | 7 |
| Iona | 64.7 | 426963.0 | 6 | -12 | -6 |
| | | 427161.0 | -11 | -3 | -14 |
| RMS | | | 15.6 cm | 15.3 cm | 5.6 cm |

1 This is ellipsoidal height difference between the GPS short distance solution and long distance s solution

2 The results with shorter distances are taken from Table 6.4 for comparison purpose.

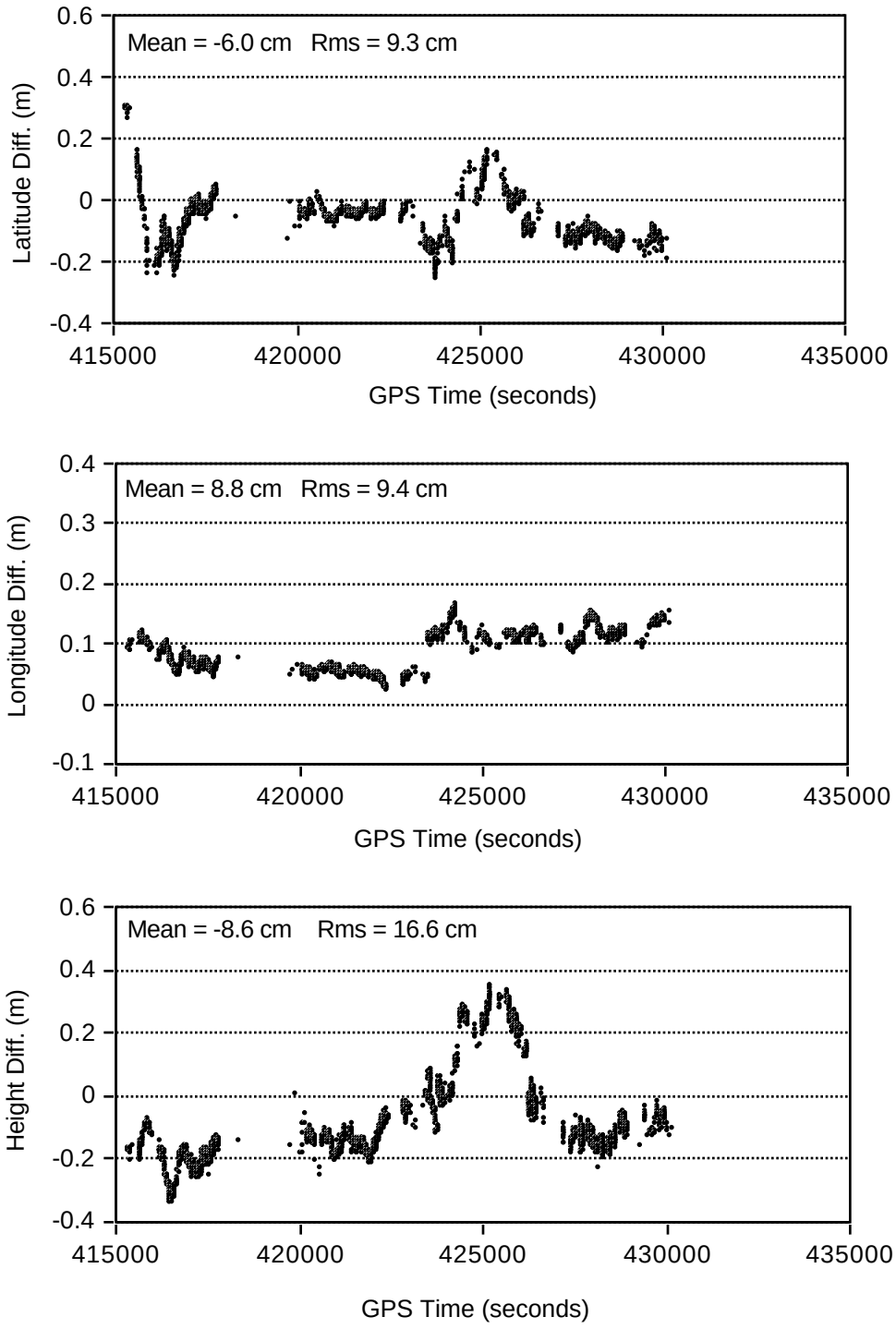


**Figure 6.11: The Launch Coordinates Differences Between Short and Long Distances**

CHAPTER 7

# CONCLUSIONS AND RECOMMENDATIONS

Precise GPS kinematic positioning using P code and narrow correlator spacing C/A code technologies in the marine environment was investigated in this thesis. Two processing methods, namely, carrier phase ambiguity resolution on the fly and carrier smoothing code, were employed. A variation of the least squares ambiguity search technique was studied and applied in three kinematic tests, two data sets collected in shipborne mode and one data set collected in land mode. In order to improve the on-the-fly ambiguity resolution time and reliability with single frequency receivers, a quadruple receiver system consisting of two static monitor units and two mobile remote units mounted on the mobile platform was tested. The results of tests carried out with a configuration of four NovAtel GPSCard™ units were analyzed and compared. The application of GPS to water level profiling with a high level of accuracy was also investigated using GPS carrier phase observations with widelane ambiguities resolved on the fly. In the following, conclusions emerging from this thesis and some recommendations for further investigations are presented.

## 7.1 CONCLUSIONS

Based on the investigations reported herein and the results obtained from the tests, major findings are as follows:

1) Both P code and narrow correlator spacing single frequency C / A code receiver technologies have same level performance in terms of ambiguity resolution on the fly in a survey launch environments when single frequency P code data is used. The observation time required for resolution is relatively long and of the order of 10 to 20 minutes.

2) The widelane (L1-L2) carrier phase observables from dual frequency P code receivers can resolve ambiguities in a few seconds. The accuracies of the solutions are slightly degraded since the receiver noise and multipath are increased in this case. However, the larger number of solutions possible results in a higher level of reliability.

3) In a survey launch environment, the multipath caused by the ship's reflective structure and sea water is a major error source. The use of chokering groundplanes proved to effectively reduce the carrier phase multipath effects. The time to ambiguity resolution could be mitigated.

4) Many factors affect the speed and reliability of ambiguity resolution on the fly, such as observation errors and biases, satellite geometry and the distance between the monitor station and the mobile remote unit. The a priori carrier phase variance is also a major factor.

5) The multi-receiver configuration approach described in this thesis to resolve the ambiguity on the fly has lead to a 45 % improvement for time to resolution compared to the use of a single pair of monitor / remote single frequency receiver. For the system consisting of four NovAtel GPSCard$^{TM}$, the ambiguity resolution on the fly is obtained in three minutes for the land kinematic case.

6) The feasibility of using GPS to establish the water profile of a river and B.M.'s along its shores with a high level of accuracy was demonstrated. The GPS error contribution is found to be 5.0 cm. The repeatability of GPS, based on re-visits of selected B.M.'s, was calculated as 5.5 cm RMS. The agreement between GPS-derived orthometric and levelled heights at B.M.'s was obtained as 6.4 cm RMS.

7) The on-the-fly ambiguity resolution using widelane observables is possible when the distances between monitor stations and remote survey launch are greater than 25 km. Distances of up to 70 km were tested in this case. The degradation of reliability for ambiguity resolution is gradual and the accuracy of water level profiling is degraded with an RMS of 15.3 cm for differences between GPS-derived and levelled (B.M.) heights when using long distances, versus 5.6 cm when using short distances. This is expected in view of the residual effects of atmosphere and orbits and the resulting difficulty in resolving the widelane ambiguities.

8) The carrier phase smoothing of the code approach is a more robust but less accurate technique. In the marine environment, the accuracy of positioning is found to be at the 50-100 cm level.

## 7.2 RECOMMENDATIONS

The research reported in this thesis is a contribution to the investigation of the performance of dual frequency P code and single frequency C/A code technologies for precise DGPS positioning in the shipborne environment and to assess the feasibility of fast and reliable on-the-fly ambiguity resolution. The following recommendations for further investigations are made:

1) In order to have more insight into the performance of the on-the-fly ambiguity resolution techniques, the effects of multipath, residual atmospheric and orbit errors and receiver noise on the performance of ambiguity resolution should be thoroughly investigated and analyzed.

2) The quadruple single frequency system for ambiguity resolution on the fly should be tested and investigated for the case of a larger platform where the antennas can be installed farther apart to decorrelate carrier phase multipath, such as in the airborne and shipborne cases. Total decorrelation is difficult to achieve on a smaller platform such as the land vehicle used in this thesis.

3) More powerful algorithms for ambiguity resolution on the fly should be investigated (e.g., Chen, 1993). With full satellite deployment, this algorithm would allow fast and reliable ambiguity resolution for all kinematic cases in all regions and during all times of the day.

4) Investigations into the effectiveness of cycle slip correction methods for the kinematic mode are required. The reliability of GPS kinematic positioning with a

high level accuracy would be improved if accurate cycle slip corrections were possible under at most operational conditions.

## REFERENCES


Abidin, H.Z. and D.W. Wells (1990): "Extrawidelaning for on-the-fly ambiguity resolution: simulation of ionospheric effects." Proceedings of the Second International Symposium on Precise Positioning with the Global Positioning System, Ottawa, Sept. 3-7, The Canadian Institute of Surveying and Mapping, pp. 1217-1232.

Abidin, H.Z. (1992): "Computational and Geometrical Aspects of On-The-Fly Ambiguity Resolution." Ph.D. Dissertation, Department of Survey Engineering Technical Report No. 164, University of New Brunswick, Fredericton, New Brunswick, Canada.

Ashjaee, J., R. Lorenz, R. Sutherland, j. Dutilloy, J. Minazio, R. Abtahi, J. Eichner, J. Kosmalska, and R. Helkey (1989) "New GPS Developments and Ashtech M-XII." Proceedings of ION GPS-89, The Institute of Navigation, Washington, D.C., pp. 195-198.

Black, H.D (1978): "An Easily Implemented Algorithm for Tropospheric Range Correction." Journal of Geophysical Research, 38(B4), pp. 1825-1828.

Cannon, M.E. (1987): "Kinematic Positioning Using GPS Pseudorange and Carrier Phase Observations. " M. Sc. Thesis, UCSE Report No. 20019, Department of Geomatics Engineering, The University of Calgary.

Cannon, M.E. (1990): "High-Accuracy GPS Semi-Kinematic Positioning: Modeling and Results." Navigation, Vol. 37, No.1, pp. 53-64.

Cannon, M.E. (1991): "Airbone GPS/INS with an Application to Aerotriangulation." Ph.D. Dissertation, UCSE Report No. 20040, Department of Geomatics Engineering, The University of Calgary.

Cannon, M.E., and G. Lachapelle (1992a): "Development of Rapid and Precise GPS Static Survey Methods." Phase I. Contract Report No. 92-001,

Geodetic Survey Division, Canada Centre for Surveying, Energy Mines and Resources, Canada.

Cannon, M.E., and G. Lachapelle (1992b): "Analysis of a High Performance C/A Code GPS Receiver in Kinematic Mode." Navigation, Vol. 39, No. 3, The Institute of Navigation, Alexandria, VA, pp. 285-299.

Cannon, M.E., J.B. Schleppe, J.F. Mclellan and T.E. Ollevier(1992c): "Real-Time Heading Determination Using an Integrated GPS-Dead Reckoning System." Proceedings of ION GPS-92, Institute of Navigation, pp. 767-773.

Chen, D.S. (1993): "Fast Ambiguity Search Filter (FASF): a Novel Concept for GPS Ambiguity Resolution" Proceedings of ION GPS-93, Salt Lake City, Sept. 22-24 (In Press).

Counselman, C.C. and S.A. Gourevitch (1981): " Miniature Interferometer Terminals for Earth Surveying: Ambiguity and Multipath with Global Positioning System." IEE Transactions on Geoscience and Remote Sensing, Vol. GE-19, No. 4, pp. 244-252.

Dewey, W. P. (1992): "Disciplined Rubidium Oscillator with GPS Selective Availability." Proceedings of ION GPS-92, Institute of Navigation, Albuquerque, NM, pp. 547-552.

Erickson, C. (1992): "Investigations of C/A Code and Carrier Measurements and Techniques for Rapid Static GPS Surveys." M. Sc. Thesis, UCSE Report No. 20044, Department of Geomatics Engineering, The University of Calgary.

Fenton, P., W. Falkenberg, T. Ford, K. Ng and A.J. Van Dierendonck (1991): "NovAtel's GPS Receiver, the High Performance OEM Sensor of the Future." Proceedings of GPS-91, The Institute of Navigation, Washington., D.C., pp. 49-58.

Frei, E. and G. Beutler (1990): "Rapid Static Positioning Based on the Fast Ambiguity Resolution Approach 'FARF': Theory and First Results." Manuscript Geodetica, Vol. 15, pp. 325-356.

Georgiadou, Y. and A. Kleusberg (1989): "Multipath effects in Static and Kinematic GPS Positioning." Proceedings of IAG International Symposium 102 on Global Positioning System: An Overview, Springer Verlag, New York, pp. 82-89.

Goad, C.C. and L. Goodman (1974): "A Modified Hopfield Troposheric Refraction Correction Model." Presented at the Fall Annual Meeting of American Geophysical Union, San Francisco, December 12-17.

Goad, C.C. (1990): "Optimal Filtering of Pseudroranges and Phases from Single-frequency GPS Receivers." Navigation, Vol. 37, No. 3, pp. 249-262.

Hatch, R. (1982): "The Synergism of GPS Code and Carrier Measurements." Proceedings of the Third International Geodetic Symposium on Satellite Doppler Positioning, Las Cruces, NM., February 8-12, DMA / NGS, Washington, D.C., pp. 1213-1232.

Hatch, R. (1991): "Instantaneous Ambiguity Resolution." Proceedings of IAG International Symposium No. 107 on Kinematic Systems in Geodesy, Surveying and Remote Sensing, Springer Verlag, New York, pp. 299-308.

Hopfield, H.S. (1969): "Two-quartic Tropospheric Refractivity Profile for Correcting Satellite Data." Journal of Geophysical Research, 74 (18), 4487-4499, 1969.

Janes, W.H., R.B. Langley, S.P. Newby (1990): "Analysis of Tropospheric Delay Prediction Models: Comparison with Ray-Tracing and Implications for GPS Relative Positioning." Submitted to Bulletin Géodésique, Oct. 1990.

Kelecy, M. T. and G. Mader (1992): "The Application of Kinematic GPS to Precise Sea Level Measurements." Proceedings of 6th International Geodetic Symposium on Satellite Positioning, Defense Mapping Agency / Ohio State University, pp. 1039-1048.

Klobuchar, J. (1983): "Ionospheric Effects on Earth-Space Propagation." Report No. ERP-866, Air Force Geophysics Laboratory, Hanscom AFB, Mass.

Lachapelle, G., W. Falkenberg, and M. Casey (1987): "Use of Phase Data for Accurate GPS Differential GPS Kinematic Positioning." Bulletin Géodésique, Intern. Ass. of Geodesy, Paris, Vol. 61, No. 4, pp. 367-377.

Lachapelle, G., W. Falkenberg, J. Hagglund, D. Kinlyside, M. Casey, P. Kielland, and H. Boudreau (1988): "Shipborne GPS Kinematic Positioning for Hydrographic Applications." Navigation, Vol. 35, No. 1, The Institute of Navigation, Alexandria, VA, pp. 73-88.

Lachapelle, G., W. Falkenberg, D. Neufeldt and P. Kielland (1989): "Marine DGPS Using Code and Carrier in Multipath Environment." Proceedings of ION GPS-89, The Institute of Navigation, Washington, D.C., pp. 343-347.

Lachapelle, G., P. Kielland and M. Casey (1991a): "GPS for Marine Navigation and Hydrography." Presented at the Fourth Biennal Canadian Hydrographic Conference, Rimouski, April 15-19.

Lachapelle, G. (1991b): "GPS Observables and Error Sources For Kinematic Positioning." Proceedings of IAG International Symposium 107 on Kinematic Systems in Geodesy, Surveying and Remote Sensing, Springer Werlag, New York, pp. 17-26.

Lachapelle, G., M.E. Cannon and G. Lu (1992): "High Precision GPS Navigation With Emphasis on Carrier Phase Ambiguity Resolution." Marine Geodesy, Taylor & Francis, Vol 15, 4, pp. 253-269.

Lachapelle, G., M.E. Cannon and G. Lu (1993a): "A comparison of P Code and High Performance C/A Code GPS Receivers for On The Fly Ambiguity Resolution." Bulletin Géodésique, Springer Verlag, New York, 67, 3, pp. 185-192.

Lachapelle, G., C. Liu, G. Lu, B. Townsend, M.E. Cannon, and R. Hare (1993b): "Precise Marine DGPS Positioning Using P Code and High Performance

C/A Code Technologies." Geomatica, Canadian Institute of Geomatics, Ottawa , 47, 2, pp. 39-46.

Lachapelle, G., C. Liu and G. Lu (1993c): "Quadruple Single Frequency Receiver System for Ambiguity Resolution on the Fly." Proceedings of ION GPS93, Salt Lake City, Sept. 22-24 (In Press).

Lachapelle, G., C. Liu, G. Lu, Q. Weigen and R. Hare (1993d): "Water Level Profiling With GPS." Proceedings of ION GPS93, Salt Lake City, Sept. 22-24 (In Press).

Landau, H., H.-J. Euler (1992): "On-the-Fly Ambiguity Resolution for Precise Differential Positioning." Proceedings of ION GPS-92, Aluquergue, NM., Sept. 16-18, The Institute of Navigation, Alexandria, VA., pp. 607-613.

Lu, G. (1991): "Quality Control for Differential Kinematic GPS Positioning." M. Sc. Thesis, UCSE Report No. 20042, Department of Geomatics Engineering, The University of Calgary.

Lu, G., M.E. Cannon, G. Lachapelle, and P. Kielland (1993): "Attitude Determination in a Survey Launch Using Multi-Antenna GPS Technology." Proceedings of National Technical Meeting, The Institute of Navigation, Alexandria, VA, 251-260.

Mader, G.L. (1990): Ambiguity Function Techniques for GPS Phase Initialization and Kinematic Solutions." Proceedings of the Second International Symposium on Precise Positioning with the Global Positioning System, Ottawa, Sept. 3-7, The Canadian Institute of Surveying and Mapping, pp. 1233-1247.

Martin, E.H. (1980): "GPS User Equipment Error Models." Global Positioning System, Volume I, Institute of Navigation, Washington, D.C.

McNeff, J.G. (1992): "NAVSTAR Global Positioning System (GPS) Signal Policy." Proceedings of ION GPS-92, Aluquergue, NM., Sept. 16-18, The Institute of Navigation, Alexandria, VA., pp. 19-22.

Pan, M., L. E. Sjöberg (1993): "Baltic Sea Level Project with GPS." Bulletin Géodésique, Springer Verlag, New York, Vol. 67, 1, pp. 51-60.

Remondi, B.W. (1984): "Using the Global Positioning System (GPS) Phase Observable for Relative Geodesy: Modeling, Processing, and Results." CSR-84-2, Center for Space Research, The University of Texas at Austin, Austin.

Remondi, B.W. (1986): "Performing centimetre-level Survey in Seconds with GPS Carrier Phase: Initial Results." Navigation, Vol. 32, No. 4, The Institute of Navigation, Alexandria, VA, pp. 386-400.

Remondi, B.W. (1991): " Kinematic GPS Results Without Static Initialization." NOAA Technical Memorandum NOS NGS-52, Rockville, MD.

Saastamoinen, J. (1973): "Contributions to the Theory of Atmospheric Refraction." Bulletin Géodésique, V 105-107, pp. 279-298, 283-297, 13-34.

She, B. (1993): "A PC-Based Unified Geoid for Canada." MSc Thesis, Report UCGE #20051, Department of Geomatics Engineering, The University of Calgary.

Van Dierendonck, A.J., P. Fenton and T. Ford (1992): "Theory and Performance of Narrow Correlator Spacing in a GPS Receiver." Vol. 39, No. 3, The Institute of Navigation, Alexandria, VA, pp. 265-283.

Veronneau, M., and A. Mainville (1992): "Computation of a Canadian Geoid Model Using the FFT Technique to Evaluate Stoke's and Vening Meinesz in a Planar Approximation." Internal Report, Geodetic Survey of Canada, Canada Centre for Surveying, Ottawa.

Weigen, Q., G. Lachapelle and M.E. Cannon (1993): "Ionospheric Effect Modelling For Single Frequency GPS Users." Submitted to Manuscripta Geodaetica.

Wells, D.E., N. Beck, D. Delikaraoglou, A. Kleusberg, E.J. Krakiwsky, G. Lachapelle, R.B. Langley, M. Nakiboglu, K.P. Schwarz, J.M. Tranquilla, P. Vanicek (1986): "Guide to GPS Positioning." Canadian GPS Associates, Fredericton, N.B..

Wübbena, G. (1989): "The GPS Adjustment Software Package GEONAP: Concepts and Models." Proceedings of 5th International Geodetic Symposium on Satellite Positioning, Physical Science Laboratory, New Mexico State University, Las Cruces, N.M., March 13-17, Vol. 1, pp. 452-461.